

# Preparation of Fullerenes and Fullerene-Based Materials

CHARLES M. LIEBER  
CHIA-CHUN CHEN

*Division of Applied Sciences and Department of Chemistry  
Harvard University  
Cambridge, Massachusetts*

I. Introduction .....	109
II. Fullerene Clusters .....	112
1. Formation of Fullerenes .....	112
2. Separation of Pure Clusters .....	117
3. Fullerene Characterization .....	121
4. Isotopically Substituted Fullerenes .....	125
III. Metal-Doped C <sub>60</sub> Materials .....	128
5. C <sub>60</sub> Solids and Thin Films .....	128
6. Considerations for Metal Doping .....	133
7. Alkali Metal-Doped Fullerenes .....	134
8. Alkaline Earth-Doped C <sub>60</sub> .....	140
9. New Directions .....	141
IV. New Fullerene Building Blocks .....	142
10. Endohedral Metal Fullerenes .....	142
11. Carbon Nanotubes .....	145
V. Concluding Remarks .....	147

## I. Introduction

Revolutionary rather than evolutionary advances in condensed matter research often arise from the discovery of new materials. The discovery of the first high temperature copper oxide superconductor, La<sub>2-x</sub>Ba<sub>x</sub>CuO<sub>4</sub>, by Bednorz and Müller in 1986<sup>1</sup> is an excellent example. This discovery initiated an explosion of research activity that has resulted in the development of many new classes of copper oxide superconductors with critical temperatures (*T<sub>c</sub>*) approaching 130 K. Most advances since

<sup>1</sup>J. G. Bednorz and K. A. Müller, *Z. Phys. B* **64**, 187 (1986).

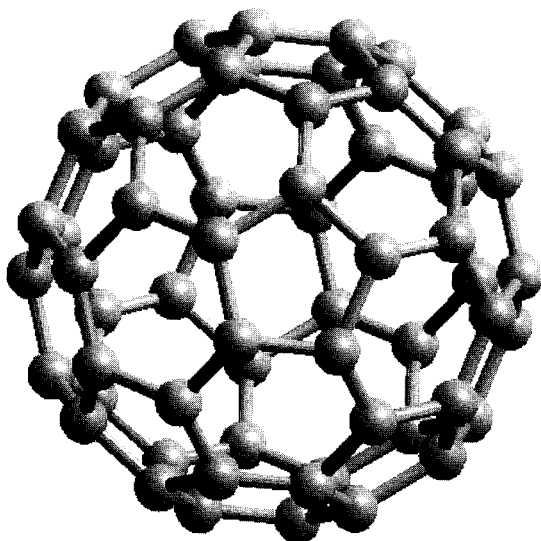


FIG. 1. Molecular structure of Buckminsterfullerene.

this revolutionary period of rapidly increasing  $T_c$ 's have been evolutionary, however, in the sense that our understanding of the high temperature copper oxide superconductors has occurred in small steps as a result of increasingly refined measurements on higher and higher quality materials. More recently, the discovery of methods to prepare and isolate macroscopic quantities of pure carbon clusters such as  $C_{60}$  has resulted in another revolution in materials physics and chemistry research.<sup>2</sup> It is this rapidly growing area of research on which we will focus in this chapter.

Historically, Smalley and coworkers first detected  $C_{60}$  as an unusually abundant species in mass spectra recorded on carbon clusters produced by laser vaporization of graphite in a helium flow.<sup>3</sup> To account for the unusually high abundance and apparent stability of the  $C_{60}$  species they proposed that the 60 carbon atoms were arranged in the shape of the truncated icosahedron or soccer ball, where each of the 60 carbon atoms has an identical environment (Fig. 1). This proposed structure, which consists of 20 hexagonal and 12 pentagonal carbon rings was inspired in

<sup>2</sup>W. Kratschmer, L. D. Lamb, K. Fostiropoulos, and D. R. Huffman, *Nature* **347**, 354 (1990).

<sup>3</sup>H. W. Kroto, J. R. Heath, S. C. O'Brien, R. F. Curl, and R. E. Smalley, *Nature* **318**, 162 (1985).

part by earlier architectural structures, geodesic domes, designed by R. Buckminster Fuller.<sup>4</sup> It is this inspiration that led to the naming of  $C_{60}$  as Buckminster-fullerene or Bucky-Ball for short. Interestingly, Euler proved in the 18th century that a closed cage or cluster made up of only hexagons and pentagons must always contain 12 pentagons, but can have any number of hexagons greater than or equal to 2. The general class of carbon clusters described by this rule are now called the fullerenes.

Smalley and coworkers<sup>3,5-7</sup> and others<sup>8,9</sup> provided significant experimental and theoretical evidence supporting the proposed soccer-ball structure of  $C_{60}$ . Prior to 1990, however,  $C_{60}$  was not a molecule you could collect in a bottle and use to make materials. The laser vaporization techniques that had been used to study  $C_{60}$  and other fullerenes produced only on the order of  $10^4$  clusters, a far cry from the  $>10^{18}$  clusters needed for a 1-mg sample of solid. Hence, the discovery by Krätschmer, Huffman, and coworkers<sup>2</sup> of a method to prepare macroscopic quantities of  $C_{60}$  and other fullerenes represents a remarkable advance that has provided the raw material fueling an explosion of materials research by physicists, chemists, and materials scientists.<sup>10-16</sup> For example, a number of fullerene-based conductors and superconductors have been prepared and intensively studied (see the chapter on fullerene superconductivity).<sup>12</sup> In addition,  $C_{60}$ -based solids that exhibit interesting optical and magnetic properties are beginning to emerge from this work.<sup>17-21</sup> Clearly, the

<sup>4</sup>R. B. Fuller, "Inventions: The Patented Works of Buckminster Fuller." St. Martin's Press, New York, 1983.

<sup>5</sup>S. C. O'Brien, J. R. Heath, R. F. Curl, and R. E. Smalley, *J. Chem. Phys.* **88**, 220 (1988).

<sup>6</sup>J. R. Heath, R. F. Curl, and R. E. Smalley, *J. Chem. Phys.* **87**, 4236 (1987).

<sup>7</sup>R. F. Curl and R. E. Smalley, *Science* **242**, 1017 (1988).

<sup>8</sup>E. A. Rohlfing, D. M. Cox, and A. Kaldor, *J. Chem. Phys.* **81**, 3322 (1984).

<sup>9</sup>H. Kroto, *Science* **242**, 1139 (1988).

<sup>10</sup>R. E. Smalley, *Acc. Chem. Res.* **25**, 98 (1992).

<sup>11</sup>J. E. Ficher, P. A. Heiney, and A. B. Smith, *Acc. Chem. Res.* **25**, 115 (1992).

<sup>12</sup>A. F. Hebard, *Phys. Today* **45**, 26 (1992).

<sup>13</sup>F. Diederich and R. L. Whetten, *Acc. Chem. Res.* **25**, 119 (1992).

<sup>14</sup>R. C. Haddon, *Acc. Chem. Res.* **25**, 127 (1992).

<sup>15</sup>P. J. Fogan, J. C. Calabrese, and B. Malone, *Acc. Chem. Res.* **25**, 134 (1992).

<sup>16</sup>J. H. Weaver, *Acc. Chem. Res.* **25**, 143 (1992).

<sup>17</sup>H. Yonehara and C. Pac, *Appl. Phys. Lett.* **61**, 575 (1992).

<sup>18</sup>Y. Wang, *Nature* **356**, 585 (1992).

<sup>19</sup>B. Miller, J. M. Rosamilia, G. Dabbagh, R. Tycko, R. C. Haddon, A. J. Muller, W. Wilson, D. W. Murphy and A. F. Hebard, *J. Am. Chem. Soc.* **113**, 6291 (1991).

<sup>20</sup>Y. Wang and L. T. Cheng, *J. Phys. Chem.* **96**, 1530 (1992).

<sup>21</sup>P. M. Allemand, K. C. Khemani, A. Koch, F. Wudl, K. Holczer, S. Donovan, G. Grüner, J. D. Thompson, *Science* **253**, 301 (1991).

preparation of macroscopic quantities of fullerenes appears to have provided a revolutionary advance in solid state research.

In this chapter, we will provide the background needed to prepare, isolate, and characterize fullerene clusters, as well as solids based on these clusters. Our goal is to provide physicists and chemists with the information needed to carry out experimental research starting only from carbon rods. First, several techniques that are used to prepare crude mixtures of fullerenes, and isolate and characterize pure  $C_n$  clusters will be reviewed. Approaches for preparing isotopically substituted clusters, which are materials essential for physical studies, will also be discussed. We will then review the properties of solid  $C_{60}$  and discuss in detail doping of solid  $C_{60}$  with different metal species. Lastly, the status and prospects of several new fullerene building blocks, including endohedral metal clusters and carbon nanotubes, will be reviewed.

## II. Fullerene Clusters

To carry out well-defined studies of fullerene-based materials requires at the very least macroscopic quantities of pure fullerene clusters. In this section we will first review methods that can be used to generate mixtures of fullerene clusters and the relative merits of these different methodologies. Effective techniques for the isolation of pure  $C_n$  ( $n = 60, 70, \dots$ ) clusters and the characterization of these large molecular species will then be discussed. Finally, we will review techniques that can be used to prepare isotopically substituted fullerenes.

### 1. FORMATION OF FULLERENES

#### a. *Arc Vaporization of Graphite*

The fullerene field was revolutionized by the discovery that simple resistive vaporization of graphite rods could produce fullerenes in substantial yield.<sup>2</sup> This procedure, which is often termed the Krätschmer-Huffman method, is a straightforward and low cost method for generating large quantities of fullerene-containing carbon soot. A typical example of an arc vaporization fullerene generating apparatus is shown in Fig. 2. Key components of the fullerene generating apparatus include (1) high-

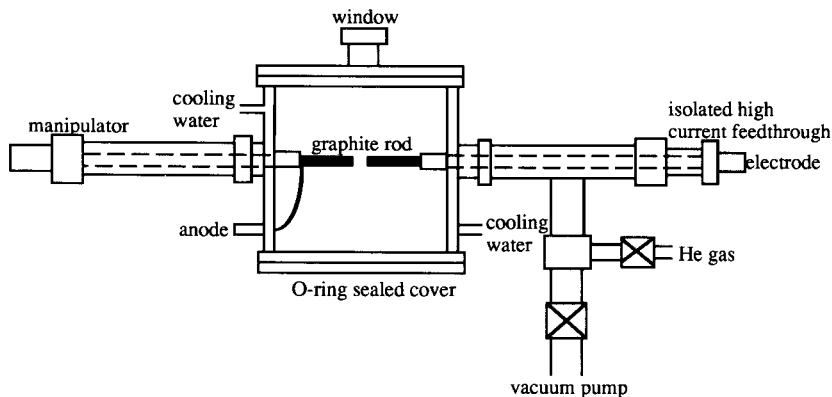


FIG. 2. Schematic illustration of the arc vaporization apparatus for generating fullerene-containing soot.

current electrical feedthroughs; (2) at least one movable electrode; and (3) a water-cooled surface to collect the vaporized carbon products. These components are housed within a vacuum chamber that is connected to a pumping/gas handling system that can evacuate the chamber to  $\leq 10^{-3}$  torr and can control the pressure between 10–500 torr. Lastly, a high current (100–200 A), low voltage AC or DC power supply is needed to drive the evaporation; an arc welder is an inexpensive but effective power supply for this purpose.

In a typical preparative experiment, two high purity graphite rods are clamped to the high current feedthroughs, and the chamber is pumped down to  $\leq 10^{-3}$  torr and refilled with He gas to a pressure of 150–250 torr. Because both oxygen and water significantly inhibit the formation of fullerenes, it is important to evacuate the chamber carefully and refill it using purified helium. The electrodes are positioned so that the carbon rods are just touching, and then the vaporization is initiated by passing a high current through the rods. For 6.25-mm-diameter rods, currents between 100 and 200 A lead to efficient fullerene formation. Under these conditions, the 6.25-mm rods are consumed at a rate of about 5–10 mm/min. The crude carbon product or soot produced by this vaporization collects on the water-cooled inner surface of the fullerene apparatus (Fig. 2) and is readily removed from the walls and collected using a stiff brush. This soot contains a variety of carbon products including  $C_{60}$  and larger fullerenes. The isolation and purification of these fullerene clusters is discussed in Section 2.

There are several experimental factors that can be varied to maximize the yield of fullerene clusters in the soot produced from the vaporization of graphite electrodes. These factors include the vaporization current density and helium partial pressure. The importance of these two experimental variables in determining the yield of fullerenes can be understood by considering the environment in which the clusters form. Specifically, the vaporization of the carbon rods is not driven by ohmic heating but rather by an arc discharge between the ends of the graphite rods. These latter conditions produce a plasma, and hence, control of temperature and cooling of the carbon plasma will determine the yield and size distribution of the fullerene clusters. Qualitatively, increases in the current density will increase the plasma temperature, while increases in the buffer gas (He) pressure will increase the cooling and growth rates of carbon species. A particularly dramatic example of the effects of He pressure is found in comparing the carbon products produced from dc discharges in 150 and 500 torr of helium. Using the former conditions fullerene clusters are observed in high yield, while at higher He pressures carbon nanotubes (see Section 11) are the principle product. Unfortunately, however, systematic studies of how the current density and the buffer gas pressure affect the yield and cluster size distribution have not been carried out. We believe that future investigations addressing these points are worthwhile, since they should provide the data needed to prepare rationally specific cluster sizes.

#### b. *Laser Ablation*

A second very useful and powerful technique for producing fullerene clusters involves laser ablation of graphite in a helium atmosphere. Historically, laser ablation was the first technique used to generate fullerene clusters in the gas phase,<sup>3,5-7</sup> although initial attempts to prepare isolable quantities of C<sub>60</sub> were unsuccessful with this technique. The early attempts to prepare fullerenes by laser ablation relied on ablation in an inert gas buffer at room temperature. The failure of these early attempts to yield macroscopic quantities of fullerenes is almost certainly due to the fact that the dense carbon plasma created during laser vaporization cools too quickly. The rapidly cooling plasma does not provide sufficient time for the growing carbon fragments to rearrange into the stable, closed fullerene structures. In support of this scenario, Smalley and coworkers first showed that laser ablation of graphite carried out at elevated temperatures could in fact lead to the efficient production of macroscopic quantities of C<sub>60</sub> and other fullerenes.<sup>9,22</sup>

A typical laser ablation apparatus that has been used to prepare

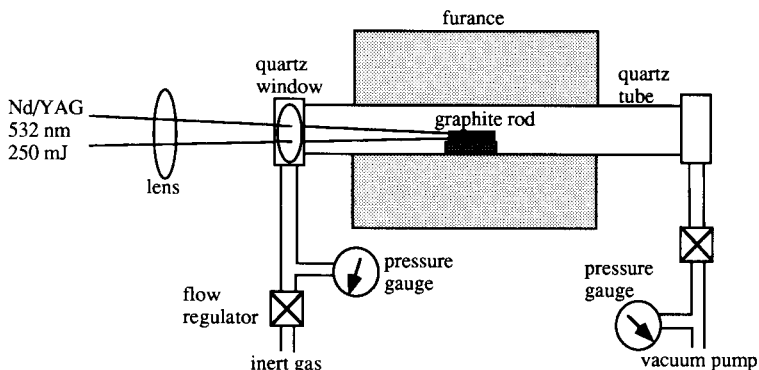


FIG. 3. Schematic view of a laser ablation apparatus for the preparation of  $C_{60}$  and other fullerenes. In this apparatus graphite is ablated inside a quartz tube held at  $1200^{\circ}\text{C}$  using the green (532 nm) line from a pulsed Nd-YAG laser. Because this procedure is carried out at elevated temperature,  $C_{60}$  and  $C_{70}$  condense at the cool end of the tube.

macroscopic quantities of fullerenes in our laboratory is shown in Fig. 3. A key feature of this apparatus is that graphite is ablated within a high temperature furnace. By carrying out the ablation at an elevated temperature, the plasma cools more slowly and growing carbon clusters have sufficient time to rearrange (anneal) into stable fullerenes. We have found that fullerene production is most efficient at  $1200^{\circ}\text{C}$ , the upper limit of our furnace. At lower temperatures, the yield of fullerenes is reduced.<sup>9,22</sup> It is possible, however, that ablation at higher temperatures (i.e.,  $>1200^{\circ}\text{C}$ ) could lead to further enhancements in the yields of fullerenes produced by this technique.

There are several features of the laser ablation method that make it an excellent technique for the preparation of fullerenes. First, it is possible to systematically vary the characteristics of the carbon plasma through variations in the laser pulse energy and wavelength.<sup>23</sup> Second, by controlling the buffer gas pressure and the furnace temperature it is also possible to control systematically the growth of clusters from the carbon plasma. Control of the growth and annealing should increase the efficiency and selectivity of the fullerenes produced. To date, these experimental variables have not been carefully explored, although such investigations could advance significantly our understanding of how to grow rationally new clusters. Finally, since the laser light is easily

<sup>22</sup>R. E. Haufler, Y. Chai, L. P. F. Chibante, J. Conceicao, C. Jin, L. S. Wang, S. Maruyama, and R. E. Smalley, *Mater. Res. Soc. Symp. Proc.* **206**, 627 (1991).

<sup>23</sup>J. T. Cheung and H. Sankur, *CRC Critical Rev. in Solid State and Mat. Sci.* **15**, 63 (1988).

positioned and no external electrical connections to the sample are needed, it is possible to produce fullerenes from very small amounts of carbon precursors. We have exploited this feature previously to prepare efficiently  $^{13}\text{C}$ -substituted fullerenes,<sup>24,25</sup> while Smalley and co-workers have used it to prepare metal-encapsulated fullerenes (see sections 4 and 10 below).

### c. Other Methods of Fullerene Production

Several other techniques, including hydrocarbon combustion, low-pressure helium sputtering, electron beam evaporation, and inductively coupled RF evaporation of graphite targets have been used to prepare fullerene containing carbon products.<sup>26-28</sup> Of these, we believe only the combustion technique is sufficiently developed to be considered as a general method for the production of macroscopic quantities of fullerenes.

The production of fullerenes from hydrocarbon combustion was first reported by Howard and co-workers in 1991.<sup>26</sup> Specifically, combustion of benzene-oxygen mixtures in laminar flow flames produced significant quantities of  $\text{C}_{60}$  and  $\text{C}_{70}$ . A maximum yield of 0.3%  $\text{C}_{60}$  and  $\text{C}_{70}$  was observed when the benzene: oxygen ratio was nearly 1 and these gases were diluted with 10% argon. Although this product yield is an order of magnitude lower than that observed for the arc-discharge and laser ablation methods of fullerene production, there are several attractive features of the flame production process. First, hydrocarbon combustion can be easily scaled-up and operated as a continuous process. These characteristics could make hydrocarbon combustion a key technique for large-scale commercial production of fullerenes. Secondly, variations in the properties of the combustion flame may be used to control systematically the size distribution fullerene clusters.<sup>26</sup> This could be useful for solid state studies of larger fullerene clusters since large clusters are only produced in low yield by the arc-discharge method. Lastly, we believe that there is great potential to investigate systematic doping of fullerene cluster using the flame method since dopants can be easily introduced into the benzene-oxygen mixture prior to combustion.

<sup>24</sup>C.-C. Chen and C. M. Lieber, *J. Am. Chem. Soc.* **114**, 3141 (1992).

<sup>25</sup>C.-C. Chen and C. M. Lieber, *Science* **259**, 665 (1993).

<sup>26</sup>J. B. Howard, J. T. McKinnon, Y. Makarovsky, A. L. Lafleur, and M. E. Johnson, *Nature* **352**, 139 (1991).

<sup>27</sup>R. F. Bunshah, S. Jou, S. Prakash, H. J. Doerr, L. Isaacs, A. Wehrsig, C. Yeretizian, H. Cynn, and F. Diederich, *J. Phys. Chem.* **96**, 6866 (1992).

<sup>28</sup>G. Peters and M. Jansen, *Angew. Chem.* **104**, 240 (1992).



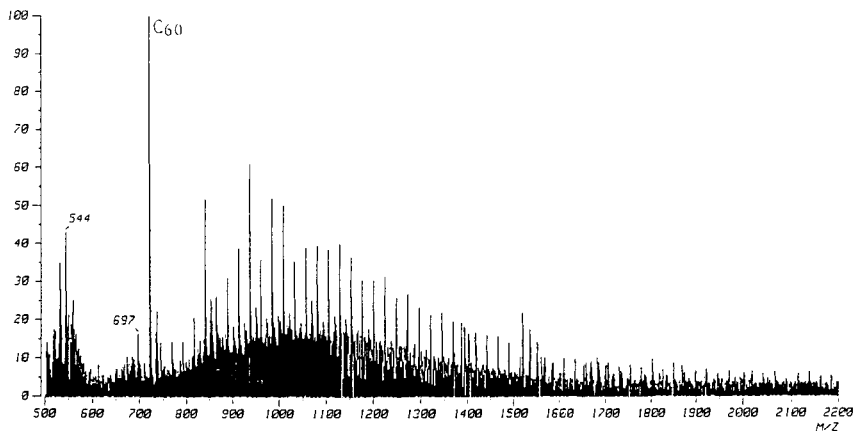


FIG. 4. Fast atom bombardment mass spectrum of the soot produced by arc vaporization of graphite rods. This spectrum illustrates the large number of different carbon products (i.e., different  $M/Z$  peaks) produced by arc vaporization.

## 2. SEPARATION OF PURE CLUSTERS

The methods of fullerene production that have been described all produce the macroscopic quantities of fullerenes needed for solid state research. In all cases, however, the fullerenes are produced as a crude mixture containing  $C_{60}$  and other  $C_n$  ( $n > 60$ ), as well as conventional hydrocarbon species (Fig. 4). In this crude soot state, the fullerenes are unsuitable for materials research. Individual fullerene clusters must be isolated from the crude soot to carry out meaningful solid state research. In this section we review several methods by which pure  $C_{60}$  and other fullerenes can be isolated from the crude soot. An overall flow chart outlining the purification procedures to be discussed is shown in Fig. 5.

The first step in most purification schemes involves the extraction of soluble fullerenes from the crude carbon soot. In the original work of Krätschmer and Huffman, benzene was used to extract  $C_{60}$  and larger fullerenes from the carbon soot.<sup>2</sup> For safety reasons, most researchers now employ toluene to extract fullerenes from soot. The extraction may be efficiently carried out using several methods. First, soot can be extracted continuously using boiling toluene in a Soxhlet solid extraction apparatus. The glassware needed for this procedure can usually be found in an organic chemistry laboratory. This method is convenient, since it can be run continuously by itself, and furthermore, completion of the procedure is readily determined when the toluene condensed in the Soxhlet extractor remains colorless. A second method that can be used to

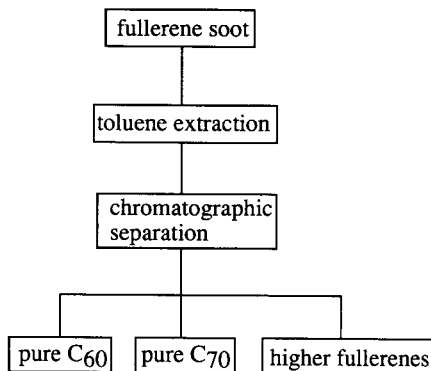


FIG. 5. Flow chart outlining the basic purification steps required to obtain pure C<sub>60</sub> and other fullerenes from the crude soot produced by arc vaporization.

extract fullerenes from soot involves sonication of toluene-soot mixture at room temperature. In this procedure, a flask containing a toluene suspension of soot is placed in an ultrasonic cleaning bath and sonicated for 30 to 60 minutes. The insoluble carbon products are then removed from the toluene solution of fullerenes by filtration.

The fullerene extract obtained using either of the foregoing methods amounts to approximately 15–20% by weight of the original carbon soot. Although a similar benzene extract was used by Krätschmer *et al.* to obtain the first measurements of the solid state properties of C<sub>60</sub>, we now know that this extract contains a number of different species that must be separated to obtain pure C<sub>60</sub>. The heterogeneous composition of the fullerene extract is clearly illustrated in the mass spectrum shown in Fig. 6. This spectrum shows that the dominant species in the extract are C<sub>60</sub> and C<sub>70</sub>; however, small quantities of larger fullerenes and low molecular weight hydrocarbons are also present in the extract. In what follows we describe several successful approaches for separating these fullerene and hydrocarbon species.

Hydrocarbon impurities can be conveniently separated from the extract prior to the isolation of the individual fullerenes. These impurities are believed to be primarily linear hydrocarbon chains that are known to form in carbon plasmas.<sup>29,30</sup> The removal of the hydrocarbons is based on the large difference in solubility of the hydrocarbons versus the fullerenes in ether: the hydrocarbon impurities are soluble in diethyl ether, while the fullerenes are essentially insoluble. Hence, to remove these

<sup>29</sup>G. V. Helden, N. G. Gotts and M. T. Bowers, *Nature* **363**, 60 (1993).

<sup>30</sup>R. F. Curl, *Nature* **363**, 14 (1993).

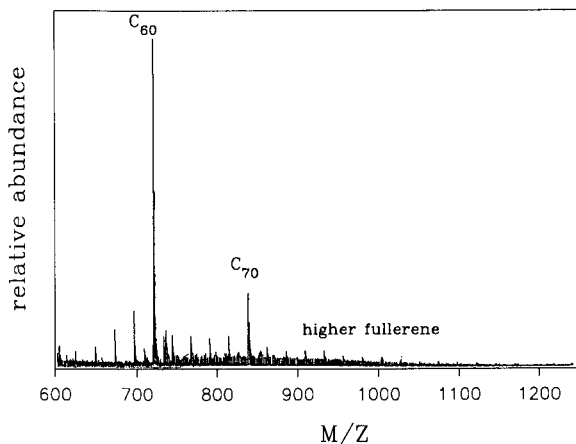


FIG. 6. Fast atom bombardment mass spectrum of the toluene soluble extract from the soot. The primary products in this extract are  $C_{60}$  and  $C_{70}$ .

impurities the toluene–fullerene extract is evaporated to dryness using a rotary evaporator, and then the resulting black solid, which contains primarily fullerenes, is washed extensively with diethyl ether to selectively remove the hydrocarbons. The solid that remains after washing contains only fullerenes.

In general, all successful schemes used to isolate pure  $C_{60}$  and other individual fullerenes utilize a chromatographic separation. The most widely used chromatographic separation employs a neutral alumina ( $Al_2O_3$ ) stationary phase and simple gravity feed.<sup>31–34</sup> Typically, a crude mixture of fullerenes is loaded onto the top of the alumina column and then eluted with 95:5 hexane:toluene mixture. An advantage of this chromatographic separation is that the progress can be monitored visually. In a good separation, at least three distinct bands can be observed during the 5% toluene elution. A purple band corresponding to  $C_{60}$  has the highest mobility and can be isolated first from the fullerene mixture. The pure  $C_{60}$  band will separate completely from other fullerene bands in a good column, and it can be eluted using the 5% toluene

<sup>31</sup>A. S. Koch, K. C. Khemani, and F. Wudl, *J. Org. Chem.* **56**, 4543 (1991).

<sup>32</sup>F. Diederich, R. Ettl, Y. Rubin, R. L. Whetten, R. Beck, M. Alvarez, S. Anz, D. Sensharma, F. Wudl, K. C. Khemani, and A. Koch, *Science* **252**, 548 (1991).

<sup>33</sup>H. Ajie, M. M. Alvarez, S. J. Anz, R. D. Beck, F. Diederich, K. Fostiropoulos, D. R. Huffman, W. Kratschmer, Y. Rubin, K. E. Schriver, D. Sensharma, and R. L. Whetten, *J. Phys. Chem* **94**, 8630 (1990).

<sup>34</sup>P. Bhyrappa, A. Penicaud, M. Kawamoto, and C. A. Reed, *J. Chem. Soc., Chem. Commun.* 936 (1992).

solution. A deep red band that corresponds to  $C_{70}$  is the second band that separates using the 5% toluene solution. To elute the  $C_{70}$  from the alumina column efficiently, however, requires an increase in the toluene:hexane ratio to approximately 1:1. The third yellow band, which has the lowest mobility on the alumina column, corresponds to a mixture of  $C_{76}$ ,  $C_{84}$ ,  $C_{90}$ , and  $C_{94}$  fullerenes.<sup>32</sup> Since these larger fullerenes constitute only a small fraction (<10%) of the crude fullerene mixture, we will not discuss the isolation of these fullerenes here. Increases in the fraction of large fullerenes are needed before these clusters will be useful for general solid state studies.

Chromatography on alumina provides a straightforward method for isolating pure  $C_{60}$  and  $C_{70}$ ; however, it also has several drawbacks. First, the separation procedure is very time consuming and requires at least several days to produce gram quantities of pure  $C_{60}$ . Second, this separation procedure requires significant quantities of organic solvents and alumina, and it produces large quantities of organic wastes. For example, it has been estimated that the purification of 1 g of  $C_{60}$  requires approximately 10 kg of alumina and 50 L of solvent.<sup>35</sup> To reduce the consumption of costly solvents and alumina, several groups have developed alumina columns within Soxhlet extractors.<sup>36,37</sup> This modified procedure has the advantage of continuously recirculating the hexane solvent; however, it only separates about 50% of the total  $C_{60}$  from the crude fullerene extract.

A newer and perhaps more attractive separation procedure has recently been reported by Tour and coworkers.<sup>35-38</sup> In this chromatographic separation, the stationary phase is activated charcoal supported on silica gel and the mobile phase is pure toluene. An important feature of this system is that material can be eluted from column under positive pressure. The positive pressure elution enables much higher solvent flows than possible using gravity feed, and thus this separation procedure is considerably faster than those based on the  $Al_2O_3$  stationary phase. Notably, with this method it is possible to obtain 1 g of pure  $C_{60}$  in less than one hour.

A final chromatography technique that can be used to separate the fullerene mixture is high pressure liquid chromatography (HPLC). HPLC instruments can be usually found in organic chemistry laboratories, and typically they have much higher separation efficiencies than the gravity

<sup>35</sup>W. A. Scrivens, P. V. Bedworth, and J. M. Tour, *J. Am. Chem. Soc.* **114**, 7917 (1992).

<sup>36</sup>K. Chatterjee, D. H. Parker, P. Wurz, K. R. Lyke, D. Gruen, and L. M. Stock, *J. Org. Chem.* **57**, 3253 (1992).

<sup>37</sup>K. C. Khemani, M. Prato, and F. Wudl, *J. Org. Chem.* **57**, 3254 (1992).

<sup>38</sup>W. A. Scrivens and J. M. Tour, *J. Org. Chem.* **57**, 6932 (1992).

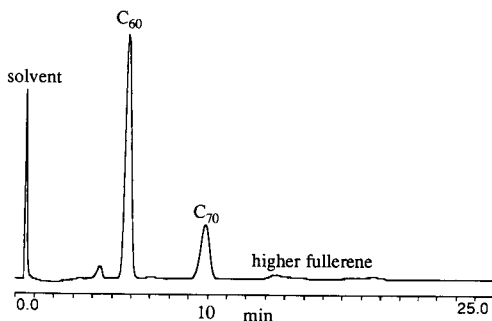


FIG. 7. HPLC chromatograph of the toluene soluble extract from the soot. The chromatograph, which corresponds to the optical density at 310 nm as a function of time, illustrates that  $C_{60}$ ,  $C_{70}$ , and higher ( $C_n$ ,  $n > 70$ ) fullerenes can be cleanly separated using this experimental technique.

and low pressure techniques already described. Typically, HPLCs also incorporate in-line absorption monitors so that it is possible to quantify the separation process as it proceeds. The optical absorption of the eluant as a function of time for a HPLC separation of a fullerene mixture is shown in Fig. 7. Clearly, the peaks corresponding to  $C_{60}$  and  $C_{70}$  are well separated under these experimental conditions. If the solution volumes corresponding to the absorption peaks were collected from successive runs, it would then be possible to isolate macroscopic quantities of  $C_{60}$  and  $C_{70}$ . A drawback of the HPLC technique is, however, that most laboratory research instruments are only equipped for milligram-scale separations. Nevertheless, it is a very convenient technique for assaying the purity of  $C_{60}$  and  $C_{70}$  samples.

### 3. FULLERENE CHARACTERIZATION

Methods used to isolate large quantities of  $C_{60}$  and  $C_{70}$  were reviewed in Section 2. These techniques can provide pure  $C_{60}$  or  $C_{70}$  that is ideal for solid state studies. It is also important, however, to verify the purity of individual samples, since impurities (e.g.,  $C_{70}$  or other hydrocarbons in  $C_{60}$ ) can significantly affect solid state properties. Here we review several techniques that can be used to verify the identity and to ascertain the purity of fullerene samples; these include (1) nuclear magnetic resonance (NMR) spectroscopy; (2) mass spectroscopy; (3) optical spectroscopy; (4) HPLC.

### a. NMR Spectroscopy

Solution phase carbon-13 NMR spectroscopy is a powerful probe of fullerene purity and structure.<sup>39-42</sup> For example, all 60 carbon nuclei are equivalent in  $C_{60}$ , and thus, a  $^{13}\text{C}$ -NMR spectrum containing purified  $C_{60}$  should exhibit only a single resonance corresponding to the pure fullerene. Indeed,  $^{13}\text{C}$  spectra recorded on  $C_{60}$  isolated using the procedure we have described show only a single resonance, at 143.2 ppm (Fig. 8).

In contrast, NMR spectra recorded on solutions of purified  $C_{70}$  exhibit five distinct resonance at 130.8, 144.4, 147.8, 148.3, and 150.8. These five resonances reflect the lower symmetry of  $C_{70}$  versus  $C_{60}$ .<sup>42</sup> The significant differences in these spectra indicate that NMR could be used to determine readily the presence of  $C_{70}$  in  $C_{60}$  samples. Consideration of the sensitivity of typical NMR instruments indicates, however, that impurities can only be detected reliably at the 1% level. Hence, observation of a single resonance in spectra of  $C_{60}$  solutions implies  $\geq 99\%$  sample purity.

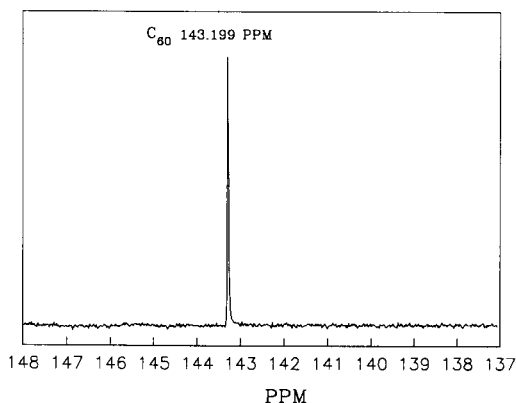


FIG. 8. Carbon-13 NMR spectrum obtained on a sample of purified  $C_{60}$  dissolved in  $C_6D_6$ . The single peak at 143.2 ppm corresponds to the 60 equivalent carbon atoms in the  $C_{60}$  cluster; the absence of other resonances in the spectrum shows that the sample contains only  $C_{60}$  at the detection limit of the NRM.

<sup>39</sup>R. Taylor, J. P. Hare, A. K. Abudl-sada, and H. W. Kroto, *J. Chem. Soc., Chem. Commun.* 1423 (1990).

<sup>40</sup>R. D. Johnson, G. Meijer, and D. S. Bethune, *J. Am. Chem. Soc.* **112**, 8983 (1990).

<sup>41</sup>C. S. Yannoni, P. P. Bernier, D. S. Bethune, G. Meijer, and J. R. Salem, *J. Am. Chem. Soc.* **113**, 3190 (1991).

<sup>42</sup>R. D. Johnson, G. Meijer, J. R. Salem, and D. S. Bethune, *J. Am. Chem. Soc.* **113**, 3619 (1991).

### b. *Mass Spectroscopy*

Another technique commonly used to determine the composition and purity of fullerene samples is mass spectroscopy. As discussed earlier, mass spectroscopy can provide a quick survey of the different fullerene clusters in carbon soot (Fig. 4). There are several important points, however, that must be considered when using mass spectroscopy as an analytical probe of sample purity. First, the evaporation and ionization process must be carefully controlled to prevent generation of new carbon species from a pure sample. For example, electron impact desorption and ionization typically results in extensive fragmentation of  $C_{60}$ . Mass spectra obtained in this way contain a host of peaks with  $m/z < 720$ , which could incorrectly indicate the presence of hydrocarbon impurities. Desorption and ionization techniques that have been used to determine reliably fullerene sample purity include field desorption and fast atom bombardment (FAB).<sup>43,44</sup> Analysis of purified  $C_{60}$  and  $C_{70}$  samples using these methods yield spectra corresponding predominantly to  $C_{60}^+$  and  $C_{70}^+$ , respectively. Another technique that has been used by several groups to produce molecular ions without significant fragmentation is laser desorption.<sup>43,45</sup> Hence, these last three techniques can be used to analyze the purity or composition of fullerene solid samples. The sensitivity of mass spectrometers to impurities is, however, dependent on a number of experimental and instrumental factors. For this reason, spectra recorded on commercial instruments generally cannot be used to assure purity to better than 99%.

### c. *Optical Spectroscopy*

Optical spectroscopy, covering the ultraviolet through infrared regions of the electromagnetic spectrum, represents a third powerful tool for characterizing fullerene clusters. Fullerenes exhibit size- and structure-dependent ultraviolet-visible (UV-VIS) absorption spectra that are due to electronic transitions within the clusters. Qualitatively, pure  $C_{60}$  solutions exhibit a deep purple color,  $C_{70}$  solutions show an intense wine red color, and higher fullerenes (i.e.,  $C_{76}$  to  $C_{94}$ ) exhibit yellow to greenish

<sup>43</sup>S. W. McElvany and M. M. Ross, *J. Am. Soc. Mass. Spectrom.* **3**, 268 (1992).

<sup>44</sup>D. M. Cox, S. Behal, M. Disko, S. M. Gorun, M. Greaney, C. S. Hsu, E. B. Kollin, J. Millar, J. Robbins, W. Robbins, R. D. Sherwood, and P. Tindall, *J. Am. Chem. Soc.* **113**, 2940 (1991).

<sup>45</sup>D. H. Parker, P. Wurz, K. Chatterjee, K. R. Lykke, J. E. Hunt, M. J. Pellin, J. C. Hemminger, D. M. Gruen, and L. M. Stock, *J. Am. Chem. Soc.* **113**, 7499 (1991).

colours.<sup>46-48</sup> These variations can be attributed to the fact that the optical transition between the highest occupied molecular orbital and lowest unoccupied molecular orbital becomes progressively smaller with increasing size, and thus the larger fullerenes absorb light at increasingly longer wavelengths.

In the specific cases of  $C_{60}$  and  $C_{70}$ , detailed features in the absorption spectra provide an unambiguous method for distinguishing between  $C_{60}$  and  $C_{70}$  or for detecting  $C_{70}$  impurities within a  $C_{60}$  sample. Representative spectra for  $C_{60}$  and  $C_{70}$  are shown in Fig. 9. The UV-VIS absorption spectrum of  $C_{60}$  exhibits strong peaks at 213, 257, and 329 nm, and weak, broad absorption between 450 and 600 nm. On the other hand,  $C_{70}$  exhibits well-defined absorption peaks at 214, 236, 331, 360, 378, and 468 nm. In comparing the  $C_{60}$  and  $C_{70}$  spectra, it is apparent that the visible absorption at 468 nm in  $C_{70}$  is one of the most clear features by which to distinguish  $C_{70}$  from  $C_{60}$  or to detect the presence of  $C_{70}$  in a  $C_{60}$  sample. Using a reference pure  $C_{60}$  spectrum, it is possible (by focusing

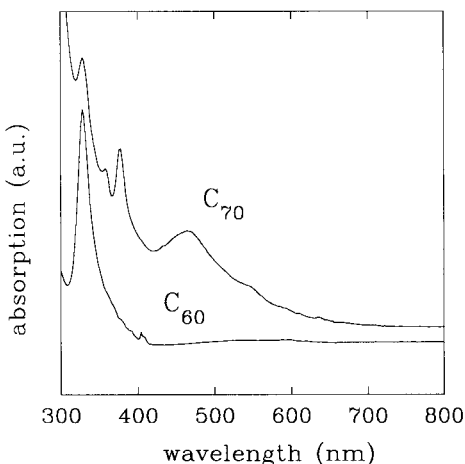


FIG. 9. Ultraviolet-visible absorption spectra of purified samples of  $C_{60}$  (bottom) and  $C_{70}$  (top) dissolved in hexane solvent. These spectra illustrate the large difference in optical density at 460 nm between  $C_{60}$  and  $C_{70}$ . This difference can be used to assess the relative purity of samples.

<sup>46</sup>R. Ettl, I. Chao, F. Diederich, and R. L. Whetten, *Nature* **353**, 149 (1991).

<sup>47</sup>L. D. Lamb, D. R. Huffman, R. K. Workman, S. Howells, T. Chen, D. Sarid, and R. F. Ziolo, *Science* **255**, 1413 (1992).

<sup>48</sup>K. Kikuchi, N. Nakahara, T. Wakabayashi, M. Honda, H. Matsumiya, T. Moriwaki, S. Suzuki, H. Shiromaru, K. Yamauchi, I. Ikemato, and Y. Achiba, *Chem. Phys. Lett.* **188**, 177 (1992).



on the region around 468 nm) to detect  $C_{70}$  impurity in an unknown  $C_{60}$  sample at the 0.1% level. Hence, optical spectroscopy is one of the most sensitive methods for determining the purity of  $C_{60}$  samples.

Infrared (IR) absorption spectroscopy is also a useful method for characterizing  $C_{60}$  and other fullerene samples. In the case of  $C_{60}$ , group theoretical analysis of the truncated icosahedron shows that there should be only 4 IR active modes for  $C_{60}$ . These four bands are experimentally observed at 1428, 1183, 577, and  $527\text{ cm}^{-1}$ . The observation of additional bands within this region thus indicates the presence of impurities in a  $C_{60}$  sample. Since strong C-H bending modes occur within this spectral region, the observation of more than four absorptions in a spectra of  $C_{60}$  typically indicates the presence of hydrocarbon impurities.

#### d. HPLC

In Section 2 we discussed the use of chromatography for isolating pure fullerene clusters. While HPLC can be used to separate macroscopic quantities of fullerenes, it is also very useful as an analytical technique for characterizing the purity of fullerene samples. For fixed experimental conditions (i.e., stationary phase, solvent, and flow rate)  $C_{60}$ ,  $C_{70}$ , and other materials elute from the column at specific and reproducible times (e.g., Fig. 6). Hence, measurements of the optical absorption as a function of time represent a straightforward assay for the presence of  $C_{70}$  (and other impurities) in a  $C_{60}$  sample. Because the intense UV bands are monitored in the HPLC experiment, it is possible to detect at least 0.1% impurities. Analytical HPLC thus represents one of the most sensitive techniques available to assess fullerene sample purity.

### 4. ISOTOPICALLY SUBSTITUTED FULLERENES

In the foregoing sections we have reviewed techniques needed to prepare, separate, and characterize fullerene carbon clusters. Before reviewing the preparation of solid materials using these pure clusters, we will discuss how the foregoing procedures can be generalized to produce modified fullerene clusters. Specifically, we discuss procedures that can be used to prepare  $C_{60}$  substituted with carbon-13. Because isotopic substitution is a powerful probe of solid state processes (see the chapter on fullerene superconductors), it is an essential topic to cover in the preparation of fullerene clusters. Here we concentrate on the preparation and characterization of  $^{13}\text{C}$  substituted  $C_{60}$ .

A number of techniques have been reported for preparing  $^{13}\text{C}$ -

substituted  $C_{60}$ ,  $(^{13}C_x ^{12}C_{1-x})_{60}$ .<sup>24,25,49-52</sup> First, holes in dense  $^{12}C$  rods have been filled with mixtures of  $^{13}C$  powder and a binder. These rods can then be vaporized using the standard arc discharge method. Since the rods contain an inhomogeneous mix of  $^{13}C$  in a  $^{12}C$  binder, and relatively large regions of pure  $^{12}C$  rod, it is not surprising that the  $C_{60}$  obtained from these rods contains a poorly controlled mass distribution as well as pure  $^{12}C_{60}$ .<sup>49-51</sup> Such inhomogeneous samples are not useful for quantitative studies of solid state properties. A second approach that appears to enable more control of  $^{13}C$  substitution was reported by Ramirez and coworkers.<sup>52</sup> In their procedure,  $^{13}C$  powder is mixed with a binder containing 90%  $^{13}C$ , the resulting viscous material is formed into a rod, and then the rod is graphitized at 2800°C. The isotopic composition of the  $C_{60}$  material obtained after arc discharge vaporization of the rods differed, however, from the calculated starting isotopic composition and contained some pure  $^{12}C_{60}$ . It is believed that the  $^{12}C$  impurities observed in the final product probably were incorporated into the rods during the high temperature graphitization step.

In contrast to the shortcomings of the foregoing procedures, we have developed a general approach that is capable of yielding reproducible  $(^{13}C_x ^{12}C_{1-x})_{60}$  samples for all values of  $x$ .<sup>24,25</sup> In this procedure a mixture of  $^{13}C$  and  $^{12}C$  powder in the desired stoichiometry ( $x$ ) is extensively ground, placed in a quartz tube between two tantalum electrodes, and then the  $^{13}C_x ^{12}C_{1-x}$  mixture is converted to dense carbon rods by resistive heating under pressure. A schematic view of the apparatus used to form these homogeneous  $^{13}C_x ^{12}C_{1-x}$  rods is shown in Fig. 10.

The dense rods produced by this procedure can be vaporized using the arc discharge<sup>24</sup> or laser ablation<sup>25</sup> techniques, although we have found that laser ablation is more efficient for the small rods produced by this method.

Because this procedure simply relies on the mixing of pure  $^{13}C$  and  $^{12}C$  powders, it is very reproducible and readily yields controlled  $^{13}C$  substitution in  $C_{60}$ . For example, the mass spectra recorded on  $C_{60}$  samples prepared from  $^{13}C_x ^{12}C_{1-x}$  rods with  $x = 1$  and  $x = 0.5$  show that the  $C_{60}$  has virtually the same mass as the starting carbon rod (Fig. 11).

<sup>49</sup>R. D. Johnson, G. Meijer, J. R. Salem, and D. S. Bethune, *J. Am. Chem. Soc.* **113**, 3619 (1991).

<sup>50</sup>J. M. Hawkins, S. Loren, A. Meyer, and R. Nunlist, *J. Am. Chem. Soc.* **113**, 7770 (1991).

<sup>51</sup>T. W. Ebbesen, J. S. Tsai, K. Tanigaki, J. Tabuchi, Y. Shimakawa, Y. Kubo, I. Hirosawa, and J. Mizuki, *Nature* **355**, 620 (1992).

<sup>52</sup>A. P. Ramirez, A. R. Kortan, M. J. Rosseinsky, S. J. Duclos, A. M. Mujsce, R. C. Haddon, D. W. Murphy, A. V. Makhija, C. M. Zahurak, and K. B. Lyons, *Phys. Rev. Lett.* **68**, 1058 (1992).

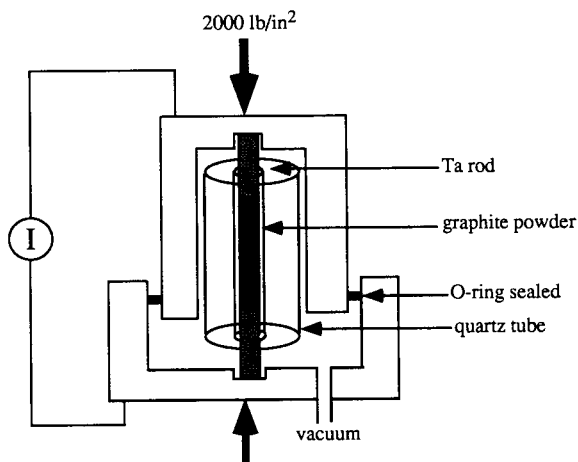


FIG. 10. Schematic illustration of the apparatus used to make dense  $^{13}\text{C}_x\text{ }^{12}\text{C}_{1-x}$  rods using mixtures of only  $^{13}\text{C}$  and  $^{12}\text{C}$  carbon powders.

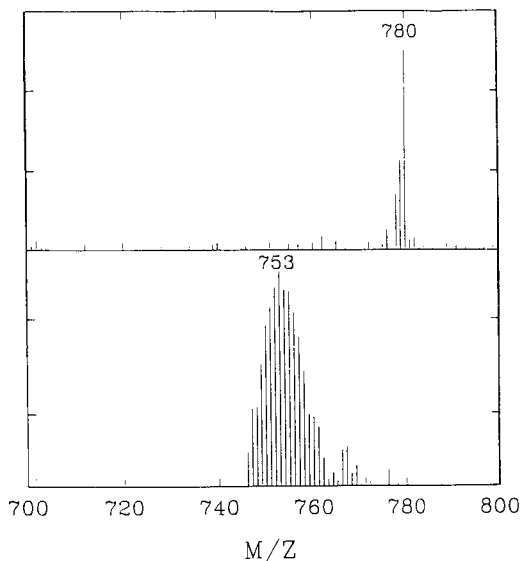


FIG. 11. Fast atom bombardment mass spectra of purified samples of  $^{13}\text{C}_{60}$  (top) and  $(^{13}\text{C}_{0.55}\text{ }^{12}\text{C}_{0.45})_{60}$  (bottom). The matrix used for the fast atom bombardment mass spectroscopy experiments was 3-nitrobenzyl alcohol.

The use of these isotopically substituted fullerenes will be discussed in detail in the chapter on fullerene superconductivity.

### III. Metal-Doped $C_{60}$ Materials

Now that the methods needed to prepare and isolate macroscopic quantities of  $C_{60}$  have been reviewed, we turn to the preparation materials based on this carbon cluster building block. In this section we will first discuss the preparation of bulk and thin film  $C_{60}$  solids. We will then review the procedures and compounds that can be prepared via metal doping reactions, and finally we will discuss new research directions.

#### 5. $C_{60}$ SOLIDS AND THIN FILMS

##### a. *Polycrystalline Powders*

Polycrystalline  $C_{60}$  is readily obtained by evaporating the solvent from  $C_{60}$  solutions. These solutions are obtained from the chromatographic purifications already described (Section 2). This material obtained directly from solvent evaporation is not suitable for solid state studies, however, since significant solvent can be trapped within the lattice. Because solvent molecules can affect the cluster packing and because these molecules may react with dopant species, it is essential to remove solvent impurities from the lattice. The most effective method for removing trapped solvent molecules from solid  $C_{60}$  involves heating the solid under vacuum. Typical conditions of temperature and pressure used for this process are 200 to 250°C and  $<10^{-3}$  torr. Importantly,  $C_{60}$  should not be dried in air, since it may be oxidized in the presence of oxygen at elevated temperature.<sup>53,54</sup>

The vacuum-dried  $C_{60}$  powder is an excellent starting material for the preparation of metal-doped solids, since it is very pure. The crystallite grain size of these powders can, however, be quite small ( $<100$  Å). Because the grain size can significantly affect solid state properties, it is important to consider methods by which the grain size can be maximized. First, the rate of solvent evaporation from the starting  $C_{60}$  solution will

<sup>53</sup>J. Milliken, T. M. Keller, A. P. Baronavski, S. W. McElvany, J. H. Callahan, and H. H. Nelson, *Chem. Mater.* **3**, 387 (1991).

<sup>54</sup>H. S. Chen, A. R. Kortan, R. C. Haddon, M. L. Kaplan, C. H. Chen, A. M. Muijsce, H. C'hou, and D. A. Fleming, *Appl. Phys. Lett.* **59**, 2956 (1991).

affect the crystal grain size; slow solvent removal promotes the growth of large crystallites. Second, extended vacuum annealing at elevated temperature promotes the growth of crystal grains. Taking into account these steps can yield polycrystalline  $C_{60}$  solids with approximately 1000 Å sized grains; however, poorly prepared samples may have crystallites as small as 60 Å. In this latter case, the granularity of the solid can severely affect the observed results (see following chapter on fullerene superconductivity).<sup>55</sup>

### b. Single Crystals

There has also been considerable effort directed toward the growth of high quality single crystals of  $C_{60}$ . This work represents an important area of research, since measurements made on single crystals often provide the deepest insight into physical properties.

In general, two approaches have been taken to grow  $C_{60}$  single crystals. The first, which is based on the original work of Krätschmer and Huffman, involves growth of the crystals from a supersaturated solution.<sup>2,56,57</sup> Using this method it is possible to obtain crystals with dimensions in excess of 1 mm. Unfortunately, these crystals generally consist of  $C_{60}$  co-crystallized with the solvent from which they were grown. Co-crystallized solvent may change the crystal structure of the solid  $C_{60}$ ,<sup>2,11,56</sup> and furthermore, it may react with metal dopants. Hence, we believe that solution phase growth is not a useful method for preparing pure  $C_{60}$  crystals that can be used in detailed physical studies.

A second technique better suited to preparation of high quality, pure  $C_{60}$  crystals involves vapor phase growth.<sup>58-61</sup> Briefly, purified and vacuum-dried  $C_{60}$  powder is sealed in a quartz tube, either under vacuum or with an inert gas such as argon, and then this tube is placed in a gradient furnace with the source end at approximately 600°C and the

<sup>55</sup>T. T. M. Palstra, R. C. Haddon, A. F. Hebard, and J. Zaanen, *Phys. Rev. Lett.* **68**, 1054 (1992).

<sup>56</sup>R. M. Fleming, A. R. Kortan, B. Hessen, T. Siegrist, F. A. Thiel, P. Marsh, R. C. Haddon, R. Tycko, G. Dabbagh, M. L. Kaplan, and A. M. Mjssce, *Phys. Rev. B* **44**, 888 (1991).

<sup>57</sup>Y. Yoshida, T. Arai, and H. Suematsu, *Appl. Phys. Lett.* **61**, 1043 (1992).

<sup>58</sup>R. L. Meng, D. Ramirez, X. Jiang, P. C. Chow, C. Diaz, K. Matsuishi, S. C. Moss, P. H. Hor, and C. W. Chu, *Appl. Phys. Lett.* **59**, 3402 (1992).

<sup>59</sup>X. D. Xiang, J. G. Hou, G. Briceno, W. A. Vareka, R. Mostovoy, A. Zettl, V. H. Crespi, and M. L. Cohen, *Science* **256**, 1190 (1990).

<sup>60</sup>C. Wen, J. Li, K. Kitazawa, T. Aida, I. Honma, H. Komiyama, and K. Yamada, *Appl. Phys. Lett.* **61**, 2162 (1992).

<sup>61</sup>J. Li, S. Komiya, T. Tamura, C. Nagasaki, J. Kihara, K. Kishio, and K. Kitazawa, *Physics C* **195**, 205 (1992).

growth end at about 500°C. After one week of growth under these conditions, it is possible to isolate pure single crystals with dimensions of up to 1 mm on edge.

### c. Thin films

There has also been considerable effort directed toward the growth of high quality  $C_{60}$  thin films since such samples are ideally suited for many physical measurements.<sup>62-68</sup> Because  $C_{60}$  sublimes at relatively low temperatures, it is straightforward to deposit thin films of this material. Early thin film growth studies utilized crude  $C_{60}/C_{70}$  mixtures as a source material under the assumption that the more volatile  $C_{60}$  would be preferentially deposited during evaporation.<sup>2,62,68</sup> Subsequent scanning tunneling microscopy (STM) studies indicate, however, that  $C_{70}$  is incorporated into the films.<sup>62</sup> Since  $C_{70}$  "impurities" may significantly affect transport and other properties, this method of film preparation is unsuitable for high quality physical studies.

More recently,  $C_{60}$  films have been deposited using pure  $C_{60}$  source material in high and ultrahigh vacuum.<sup>65-67</sup> Crystalline films have been grown on a variety of substrates (e.g., KBr, glass, or Si) with source temperatures between 573 and 773 K and the substrate at ambient (300 K) temperature. X-ray diffraction and STM structural analyses of films grown at 300 K indicate that these materials consist of randomly oriented crystalline domains with sizes ranging from 50 to 150 Å. The granular character of these films has important consequences in the interpretation of transport measurements (see the chapter on fullerene superconductivity).

Several strategies have been investigated to reduce the granularity of  $C_{60}$  thin films. First, depositions have been carried out with the substrates at elevated temperatures.<sup>67,68</sup> Structural studies of films deposited on

<sup>62</sup>R. J. Wilson, G. Meijer, D. S. Bethune, R. D. Johnson, D. D. Chambliss, M. S. de Vries, H. E. Hunziker, and H. R. Wendt, *Nature* **348**, 621 (1990).

<sup>63</sup>A. F. Hebard, R. C. Haddon, R. M. Fleming, and A. R. Kortan, *Appl. Phys. Lett.* **59**, 2109 (1991).

<sup>64</sup>P. Dietz, K. Fostiropoulos, W. Krätschmer, and P. K. Hansma, *Appl. Phys. Lett.* **60**, 62 (1992).

<sup>65</sup>G. P. Kochanski, A. F. Hebard, R. C. Haddon, and A. T. Fiory, *Science* **255**, 184 (1992).

<sup>66</sup>Y. Z. Li, J. C. Patrin, M. Chander, J. H. Weaver, L. P. F. Chibante, and R. E. Smalley, *Science* **252**, 547 (1991).

<sup>67</sup>Y. Z. Li, M. Chander, J. C. Patrin, J. H. Weaver, L. P. F. Chibante, and R. E. Smalley, *Science* **253**, 429 (1991).

<sup>68</sup>D. Schmicker, S. Schmidt, J. G. Skofronick, J. P. Toennies, and R. Vollmer, *Phys. Rev. B* **44** 10995 (1991).

substrates heated between 400 and 500 K show that elevated temperature growth enhances grain size. Because the upper temperature limit for growth is limited by the relatively low sublimation temperature of  $C_{60}$ , it is unclear how much film quality will be improved using this strategy. A second approach to improving film quality involves growth on a lattice-matched substrate. For example, Schmicher *et al.* have reported epitaxial growth of  $C_{60}$  monolayers on cleaved mica surfaces at 300 K<sup>68</sup>; the tensile strain in the monolayer was 1% based on the bulk  $C_{60}$  lattice parameters. Although this result is promising, it is uncertain how well epitaxial growth can be sustained in multilayer films of this van der Waals solid. Further studies of the growth of  $C_{60}$  films on lattice-matched substrates at different growth temperatures are clearly needed to advance this area.

#### d. $C_{60}$ Structure

The structural properties of  $C_{60}$  solids will be reviewed in detail in the chapter by Axe, Moss, and Neumann. Here we briefly introduce key features of solid  $C_{60}$  that are important to understand metal doping of this solid.

On the basis of x-ray, neutron, and electron diffraction studies it is now well established that  $C_{60}$  crystallizes in a face-centered cubic (fcc) lattice with a lattice constant of 14.17 Å at room temperature (Fig. 12).<sup>11,69-74</sup> In this structure the separation between nearest neighbor  $C_{60}$  clusters is 10 Å. The distance between adjacent 7.1-Å-diameter  $C_{60}$  molecules is thus 2.9 Å. Interestingly, comparison of this intercluster separation with the 3.35-Å interplanar separation in graphite indicates that the  $C_{60}$  clusters may be more strongly coupled than the carbon planes in graphite after normalizing for the contact area.

An important feature of an fcc structure made up from these relatively large, spherical clusters is that there are sizable, well-defined intercluster holes within the lattice. These holes constitute 26% of the total cell

<sup>69</sup>S. Liu, Y.-J. Lu, M. M. Kappes, and J. A. Ibers, *Science* **254**, 408 (1991).

<sup>70</sup>P. A. Heiney, J. E. Fisher, A. R. McGhie, W. J. Romanow, A. M. Denenstein, J. P. McCauley, and A. B. Smith, *Phys. Rev. Lett.* **66**, 2911 (1991).

<sup>71</sup>J. E. Fisher, P. A. Heiney, A. R. McGhie, W. J. Romanow, A. M. Denenstein, J. P. McCauley, and I. A. B. Smith, *Science* **252**, 1288 (1991).

<sup>72</sup>W. I. F. David, R. M. Ibberson, J. C. Matthewman, K. Prassides, T. J. S. Dennis, J. P. Hare, H. W. Kroto, R. Taylor, and D. R. M. Walton, *Nature* **353**, 147 (1991).

<sup>73</sup>D. A. Neumann, J. R. D. Copley, R. L. Cappelletti, W. A. Kamitakara, R. M. Lindstrom, K. M. Creegan, D. M. Cox, W. J. Romanow, N. Coustel, J. P. McCauley, Jr., N. C. Maliszewskyj, J. E. Fischer, and A. B. Smith III, *Phys. Rev. Lett.* **67**, 3808 (1991).

<sup>74</sup>J. Q. Li, Z. X. Zhao, D. B. Zhu, Z. Z. Gan, and D. L. Yin, *Appl. Phys. Lett.* **59**, 3108 (1991).

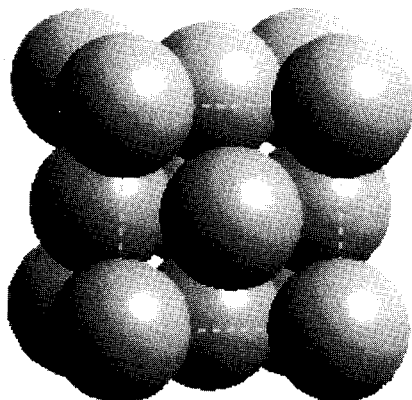


FIG. 12. Model illustrating the packing of individual clusters in the fcc lattice solid  $C_{60}$ . The  $C_{60}$  clusters are represented by gray shaded spheres in this model.

volume. On a per  $C_{60}$  basis, there is one octahedral hole and two tetrahedral holes (Fig. 13). These octahedral and tetrahedral holes have radii of 2.06 and 1.12 Å, respectively, and thus these spaces can in principle accommodate a large variety of species without a change in the basic  $C_{60}$  structure. In the next section we discuss general considerations for the preparation of metal-doped  $C_{60}$  solids and review specific compounds formed using alkali and alkaline earth metal dopants.

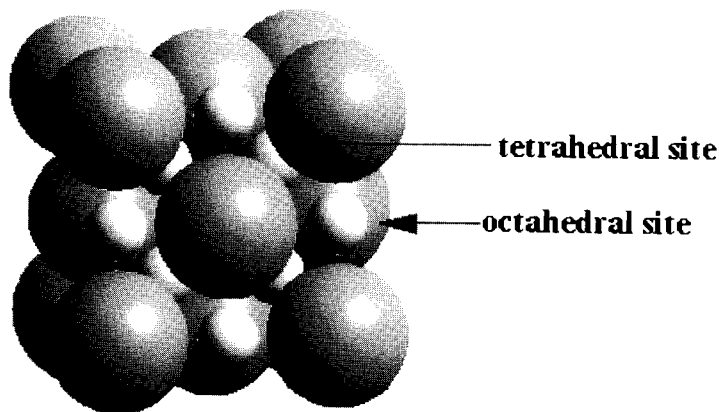


FIG. 13. Model illustrating the packing in the alkali metal-doped  $M_3C_{60}$  fcc solid. The alkali metal dopants, which are represented by light gray shaded spheres, fill the octahedral and tetrahedral holes that exist in the fcc  $C_{60}$  lattice.



## 6. CONSIDERATIONS FOR METAL DOPING

Both the octahedral and tetrahedral sites can in principle accommodate metal dopant species. The process of adding metals to these lattice holes in solid  $C_{60}$  is similar in many respects to the intercalation of metals and other species into the interlayer region of graphite. Hence, it is reasonable to utilize procedures developed for the preparation of graphite intercalation compounds as a starting point for the preparation of metal-doped  $C_{60}$  solids.

One of the most common procedures for preparing graphite intercalation compounds involves vapor phase diffusion of a volatile dopant species into the interplanar regions of the solid. Not surprisingly, vapor phase diffusion also constitutes one of the most successful methods used to prepare high quality metal-doped  $C_{60}$  samples.

In general, there are several important issues to consider in the vapor phase doping process. First, successful intercalation into the holes in the  $C_{60}$  lattice requires that the metal dopant exhibit significant vapor pressure at a temperature below which the metal reacts with  $C_{60}$  and below which  $C_{60}$  decomposes. Second, the diffusion of dopants within crystallites of a solid  $C_{60}$  is much slower than previously found in graphite intercalation compounds. This behavior is due to the fact that the dopant ions in  $C_{60}$  must hop between well-separated hole sites in the lattice versus a simple two-dimensional diffusion through interlayer regions in graphite. A schematic view of how the metal doping process is believed to proceed in polycrystalline  $C_{60}$  samples is illustrated in Fig. 14. In this general model, vapor phase metal initially condenses around the grains in the solid. Extensive annealing is then needed to achieve an equilibrium distribution of metal dopant ions within the lattice. Notably, this model suggests that it may be very difficult to achieve uniform doping in single

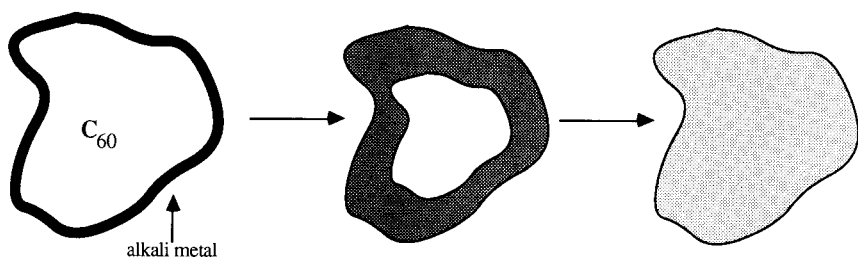


FIG. 14. Schematic view of the "vapor phase" doping process. Initially, alkali metal vapor deposits as a layer on  $C_{60}$  grains, and then this metal diffuses into the solid.

crystal samples. A final consideration in working with metal-doped  $C_{60}$  solids is that they are air sensitive. This air sensitivity arises from the fact that metal intercalation involves charge transfer from metal to  $C_{60}$ , and thus the doped solids are highly reduced and can react with oxygen and water vapor in the atmosphere. Thus, it is essential to always handle the metal-doped  $C_{60}$  solids in an inert gas or vacuum environment. In Sections 7 and 8 we will elaborate on these points for the specific cases of alkali and alkaline earth metal-doped  $C_{60}$  solids.

## 7. ALKALI METAL-DOPED FULLERENES

Much of the initial explosion of activity in fullerene research was fueled by the reports from Bell Laboratories of conductivity and then superconductivity in potassium- and rubidium-doped  $C_{60}$ .<sup>12,14,75-78</sup> Extensive studies carried out since these initial reports have resulted in the characterization of many of the properties of the superconducting phase. These properties will be discussed in detail in the chapter on fullerene superconductivity. Here we briefly review only those properties relevant to understanding the preparation of these solids.

It is now well established that the superconducting phase of alkali metal-doped  $C_{60}$  solids is derived from the fcc  $C_{60}$  lattice by filling the single octahedral and two tetrahedral holes with metal ions. This filling yields an overall stoichiometry  $M_3C_{60}$ , where  $M$  is an alkali metal. A general structural model for the  $M_3C_{60}$  structure that highlights the octahedral and tetrahedral sites in the lattice was shown in Fig. 13. comparison of this structure with that for pure  $C_{60}$  (Fig. 12) demonstrates that doping to a 3:1  $M:C_{60}$  ratio only fills the holes in the lattice and does not result in gross structural changes.

In addition, it is possible to prepare  $C_{60}$  solids in which the  $M:C_{60}$  ratio is greater than 3:1. Specifically, compounds with stoichiometries of

<sup>75</sup>R. C. Haddon, A. F. Hebard, M. J. Rosseinsky, D. W. Murphy, S. J. Duclos, K. B. Lyons, B. Miller, J. M. Rosamila, R. M. Fleming, A. R. Kortan, S. H. Glarum, A. V. Makhija, A. J. Muller, R. H. Eick, S. M. Zahurak, R. Tycko, G. Dabbagh, and F. A. Thiel, *Nature* **350**, 320 (1991).

<sup>76</sup>A. F. Hebard, M. J. Rosseinsky, R. C. Haddon, D. W. Murphy, S. H. Glarum, T. T. M. Palstra, A. P. Ramirez, and A. R. Kortan, *Nature* **350**, 600 (1991).

<sup>77</sup>M. J. Rosseinsky, A. P. Ramirez, S. H. Glarum, D. W. Murphy, R. C. Haddon, A. F. Hebard, T. T. M. Palstra, A. R. Kortan, S. M. Zahurak, and A. V. Maikhija, *Phys. Rev. Lett.* **66**, 2830 (1991).

<sup>78</sup>P. W. Stephens, L. Mihaly, P. L. Lee, R. L. Whetten, S.-M. Huang, R. Kaner, F. Deiderich, and K. Holczer, *Nature* **351**, 632 (1991).

$M_4C_{60}$  and  $M_6C_{60}$  have been prepared and structurally characterized.<sup>12,79,80</sup> Neither of these metal-doped materials has the fcc structure of solid  $C_{60}$ , but rather both are derived from more open body-centered cells. X-ray diffraction investigations have shown that  $M_4C_{60}$  has a body-centered tetragonal (bct) cell, while  $M_6C_{60}$  adopts a body-centered cubic (bcc) structure. The unit cells for these two solids are illustrated in Fig. 15. Although the  $M_4C_{60}$  and  $M_6C_{60}$  compounds are nonsuperconducting, we mention them here since they represent well-defined compounds in the alkali-metal/ $C_{60}$  phase diagram.

A number of strategies have been proposed for the preparation of alkali metal-doped  $C_{60}$ . These are reviewed in the following subsections with an emphasis on procedures that can be used to prepare high quality  $M_3C_{60}$  superconductors.

#### a. Vapor Phase Doping

As has been indicated, vapor phase doping of  $C_{60}$  has been a popular and successful technique. The high volatility of all of the alkali metals except Li at low temperature enables doping to be carried out under mild conditions where  $C_{60}$  remains stable. A general protocol for doping is as follows: First, polycrystalline  $C_{60}$  solid is dried in vacuum at elevated temperature and then transferred to an inert atmosphere glove box. A weighed sample of  $C_{60}$  (10–30 mg) is then placed in a pyrex or quartz reaction tube, and then a stoichiometric amount of alkali metal is added to the tube. A convenient and relatively accurate method of adding the metal dopant is to use measured lengths of a glass capillary tube filled with the alkali metal. The reaction tube containing  $C_{60}$  and alkali metal are sealed with a high vacuum valve, and then are removed from the inert atmosphere chamber, evacuated, and sealed under high vacuum. The sealed reaction tubes are heated between 200 and 400°C to intercalate the alkali metal into the  $C_{60}$  lattice. Although the  $M_3C_{60}$  superconducting phase can be detected by magnetization measurements in less than 12 hours, most of the sample remains undoped, as illustrated in Fig. 14. Inhomogeneous doping is an even greater problem for single crystal samples since the surface-to-volume ratio is so small, while in thin films it appears that homogeneous doping can be achieved in a matter of minutes.<sup>65</sup>

<sup>79</sup>R. M. Fleming, M. J. Rosseinsky, A. P. Ramirez, D. W. Murphy, J. C. Tully, R. C. Haddon, T. Siegrist, R. Tycko, S. H. Glarum, P. Marsh, G. Dabbagh, S. M. Zahurak, A. V. Makhija, and C. Hampton, *Nature* **352**, 701 (1991).

<sup>80</sup>O. Zhou, J. E. Fischer, N. Coustel, S. Kycia, Q. Zhu, A. R. McGhie, W. J. Romanow, J. P. McCauley, A. B. Smith, and D. E. Cox, *Nature* **351**, 461 (1991).

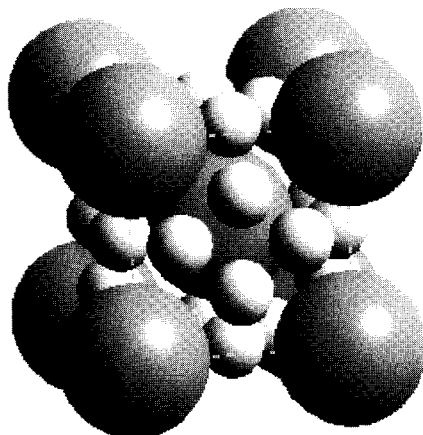
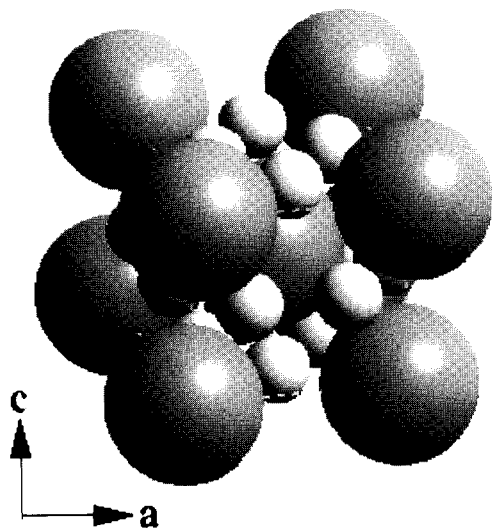


FIG. 15. Models illustrating the packing of  $C_{60}$  clusters (gray shaded spheres) alkali metal dopants (light gray shaded spheres) in the body-centered tetragonal  $M_4C_{60}$  (top) and body-centered cubic  $M_6C_{60}$  (bottom) solids.

Since preparation of samples with homogeneous dopant distributions is essential for physical studies, it is important to consider methods for improving the doping homogeneity in the vapor phase technique. A straightforward approach that has been used by several groups involves annealing at increasingly higher temperatures ranging from 250 to 400°C.<sup>81</sup> The effectiveness of this annealing technique is limited, however, by the poor contact between crystalline grains in powder samples, the stability of other nonsuperconducting phases (e.g.,  $M_4C_{60}$  and  $M_6C_{60}$ ), and sample decomposition. The contact between grains can be improved by using pressed pellet samples; however, the other limitations are intrinsic to the  $C_{60}$  system. Alternatively, vapor phase doping can be carried out with more than a six to one excess of rubidium to prepare first  $Rb_6C_{60}$ .<sup>82</sup> Because no more than six Rb ions can be intercalated into the  $C_{60}$  lattice, it is possible to synthesize  $Rb_6C_{60}$  as a well-defined, homogeneous compound. Extensive mixing and subsequent heating of equal molar ratios of  $Rb_6C_{60}$  and  $C_{60}$  can then yield good samples of  $Rb_3C_{60}$ .<sup>82</sup>

#### b. *Metal Alloys and Metal-Doped $C_{60}$*

To enhance the doping process, we proposed early on that metal alloys be used to intercalate solid  $C_{60}$ .<sup>83,84</sup> In these intercalation reactions a metal alloy such as KHg or RbHg is mixed with  $C_{60}$  and then heated in a sealed tube as described in Section 7.a. There are several features of this alloy method that make it an attractive approach for preparing metal-doped  $C_{60}$ . First, alkali-metal/Hg alloys are hard solids in comparison with pure alkali metals. It is thus possible to grind the MHg alloys into a fine powder and intimately mix this powder with the  $C_{60}$  prior to heating. Second, the increased molar mass and greater stability of the alloys (i.e., they are less reactive toward  $O_2$  and  $H_2O$  impurities) enable the stoichiometry to be controlled much more accurately than when using pure alkali metal dopants. Third, we have found that intercalation generally proceeds more rapidly at low temperature than when using pure alkali metals.<sup>84</sup> This enhanced reactivity is probably due to the intimate  $C_{60}$ /alloy mixture, since alkali metal diffusion is required within

<sup>81</sup>K. Holczer, O. Klein, S.-M. Huang, R. B. Kaner, K.-J. Fu, R. L. Whetten, and F. Diederich, *Science* **252**, 1154 (1991).

<sup>82</sup>J. P. McCauley, Q. Zhu, N. Coustel, O. Zhou, G. Vaughn, S. H. J. Idziak, J. E. Fischer, S. W. Tozer, D. M. Groski, N. Bykovetz, C. L. Lin, A. R. McGhie, B. H. Allen, W. J. Romanow, A. Denenstein, and A. B. Smith, *J. Am. Chem. Soc.* **113**, 8537 (1991).

<sup>83</sup>S. P. Kelty, C.-C. Chen, and C. M. Lieber, *Nature* **352**, 223 (1991).

<sup>84</sup>C.-C. Chen, S. P. Kelty, and C. M. Lieber, *Science* **253**, 886 (1991).

C<sub>60</sub> grains as in the case of vapor phase doping. One potential limitation of this alloy approach to doping is that components of the alloy other than the alkali metal (e.g., Hg) may be incorporated as an impurity in the C<sub>60</sub> lattice. In the case of MHg alloys this does not appear to be a major limitation, since Hg can be distilled from the solid.

In addition to the formation of K<sub>3</sub>-, Rb<sub>3</sub>-, and K<sub>3-x</sub>Rb<sub>x</sub>C<sub>60</sub> solids using K-, Rb-, and K<sub>1-x</sub>Rb<sub>x</sub>Hg alloys,<sup>84</sup> respectively, this general idea has been used to prepare other alkali metal-doped C<sub>60</sub> solids. For example, Rosseinsky and coworkers have used Na<sub>5</sub>Hg<sub>2</sub> and NaH to prepare a variety of Na<sub>x</sub>C<sub>60</sub> and Na<sub>2</sub>MC<sub>60</sub> (*M* = Cs, Rb) solids.<sup>85</sup> They found that it was possible to achieve much greater control of the sodium stoichiometry in these solids using the alloys versus the pure Na metal. More generally, we believe that low melting point alloys may represent a useful approach to explore for the preparation of C<sub>60</sub> solids doped with nonvolatile metals.

### c. Solution Phase Doping

A final approach that has been used successfully to prepare alkali-metal/C<sub>60</sub> superconductors involves reaction of C<sub>60</sub> and alkali metal in an organic solvent.<sup>86-88</sup> The motivation behind solution phase doping is that stoichiometric reduction of a homogeneous C<sub>60</sub> solution and subsequent precipitation should in principle lead to a homogeneously doped solid. Initial studies by Wang and coworkers showed that superconducting K<sub>3</sub>C<sub>60</sub> and Rb<sub>3</sub>C<sub>60</sub> could be obtained from the direct reduction of C<sub>60</sub> in toluene using an excess of K or Rb metal, respectively.<sup>86,87</sup> The fraction of the superconducting phase observed in these studies, was, however, <10%. This low yield of the superconducting phase is not surprising since C<sub>60</sub><sup>1-</sup> species are expected to precipitate as they are formed from the nonpolar solvent (toluene) used in this work. Indeed, more recent work demonstrates the MC<sub>60</sub> is the dominant phase obtained from reduction in toluene.<sup>88</sup>

<sup>85</sup>M. J. Rosseinsky, D. W. Murphy, R. M. Fleming, R. Tycko, A. P. Ramirez, T. Siegrist, G. Dabbagh, and S. E. Barrett, *Nature* **356**, 416 (1992).

<sup>86</sup>H. H. Wang, A. M. Kini, B. M. Savall, K. D. Carlson, J. M. Williams, K. R. Lykke, P. Wurz, D. H. Parker, M. J. Pellin, D. M. Gruen, U. Welp, W.-K. Kowk, S. Fleshler, and G. W. Crabtree, *Inorg. Chem.* **30**, 2838 (1991).

<sup>87</sup>H. H. Wang, A. M. Kini, B. M. Savall, K. D. Carlson, J. M. Williams, M. W. Lathrop, K. R. Lykke, D. H. Parker, P. Wurz, M. J. Pellin, D. M. Gruen, U. Welp, W.-K. Kwok, S. Fleshler, G. W. Crabtree, J. E. Schirber, and D. L. Overmyer, *Inorg. Chem.* **30**, 2962 (1991).

<sup>88</sup>J. A. Schlueter, H. H. Wang, M. W. Lathrop, U. Geiser, K. D. Carlson, J. D. Dudek, G. A. Yaconi, and J. M. Williams, *Chem. Mat.* **5**, 720 (1993).

To increase the ratio of  $M:C_{60}$  in the solid thus requires a solvent that can dissolve both  $C_{60}$  and  $C_{60}^{n-}$  ions. This solvation can be accomplished with toluene/benzonitrile mixtures, since benzonitrile can effectively solvate  $C_{60}^{n-}$  anions in solution. Hence, reduction of  $C_{60}$  in toluene/benzonitrile mixtures using either K or Rb metal and subsequent precipitation of the  $M-C_{60}$  solid yield materials with superconducting fractions in excess of 50%. Advantages of the solution phase approach to doping include (1) doping can be carried out on a large scale with little influence on the product homogeneity, and (2) the process can be carried out at significantly lower temperatures ( $<110^{\circ}\text{C}$ ) than possible with either the vapor phase or alloy methods of doping. Such low temperature doping may be utilized in the future to prepare new metastable phases. There is also a significant disadvantage to this approach, since it is known that solution phase  $C_{60}$  crystal growth traps solvent in the lattice. Hence, the presence and possible effects of trapped solvent molecules in the metal-doped  $C_{60}$  samples produced in solution must be addressed.

#### d. Alkali Metal-Doped $C_{60}$ Superconductors

As discussed in Section 5, the superconducting phase of all of the known alkali metal-doped  $C_{60}$  superconductors has a stoichiometry of  $M_3C_{60}$  and a fcc structure with the metal ions ( $M$ ) occupying the one octahedral and two tetrahedral holes in the lattice. The known superconducting phases reported to date with alkali metal dopants and the transition temperatures ( $T_c$ ) of these materials are summarized in Table I; these compounds can be prepared in high yield using either the vapor phase or alloy doping methods.

Examination of Table I shows that in addition to the pure compounds  $K_3C_{60}$  and  $Rb_3C_{60}$ , there are a number of mixed metal and/or solid solution superconductors. The total alkali metal ion to  $C_{60}$  ratio in the

TABLE I. ALKALI METAL-DOPED  
 $C_{60}$  SUPERCONDUCTORS

Material	$T_c$ (K)
$N_{a2}CsC_{60}$	10–11
$K_3C_{60}$	19.2
$K_2R_bC_{60}$	22–23
$K_2C_sC_{60}$	24
$KR_{b2}C_{60}$	26–27
$R_{b3}C_{60}$	29.4
$R_{b2}C_sC_{60}$	31

solid solution compounds is, however, always 3 : 1. There are also several notable absences from this table. First, the pure fcc phase  $\text{Cs}_3\text{C}_{60}$  has not yet been clearly observed, although bcc  $\text{Cs}_6\text{C}_{60}$  is a well-characterized solid.<sup>80</sup> It is apparent that  $\text{Cs}_3\text{C}_{60}$  is unstable relative to  $\text{Cs}_6\text{C}_{60}$  under conventional doping conditions (e.g.,  $>200^\circ\text{C}$ ) since heating 3 : 1 mixtures of Cs :  $\text{C}_{60}$  yields products containing  $\text{C}_{60}$  and  $\text{Cs}_6\text{C}_{60}$ . It may be possible, however, to trap the  $\text{Cs}_3\text{C}_{60}$  phase by doping at much lower temperatures. Since  $\text{Cs}_3\text{C}_{60}$  is expected to have a higher  $T_c$  than any known fullerene superconductor, this will be an interesting area to investigate in the future. Second, the phase  $\text{Na}_3\text{C}_{60}$ , while it exists at 300 K, is not superconducting.<sup>85</sup> It is now believed that the absence of superconductivity in this material is due to a structural phase transition below 250 K in which the material disproportionates into  $\text{Na}_2\text{C}_{60}$  and  $\text{Na}_6\text{C}_{60}$  domains. These results for the Cs and Na- $\text{C}_{60}$  phases suggest that dopant size must be carefully considered when attempting to prepare new materials. If the ions are too large for the tetrahedral holes (i.e., Cs) or if they are too small for the octahedral holes (e.g., Na), then the desired fcc structure may be unstable.

## 8. ALKALINE EARTH METAL-DOPED $\text{C}_{60}$

For the alkali metals (Li, Na, K, Rb, Cs) only  $M_3\text{C}_{60}$  fcc solids have exhibited superconductivity (Table I). The discovery of superconductivity in calcium and barium metal-doped  $\text{C}_{60}$ <sup>89-91</sup> represents, however, structurally and compositionally distinct materials in which to explore fullerene superconductivity. The alkaline earth metal-doped  $\text{C}_{60}$  superconductors are, however, considerably more difficult to prepare than the alkali metal-doped materials already discussed. This difficulty is due in large part to the low vapor pressure of the alkaline earth metals at convenient reaction temperatures. As a consequence of their low vapor pressure, solid state diffusion is the dominant mechanism by which alkaline earth metal intercalation or doping occurs in bulk  $\text{C}_{60}$ . In contrast, vapor phase diffusion accounts for the transport of alkali metals to grains in the  $\text{C}_{60}$  powder, and solid state diffusion is only required within individual crystal grains. Hence, methods that enhance solid state

<sup>89</sup>A. R. Kortan, N. Kopylov, S. Glarum, E. M. Gyorgy, A. P. Ramirez, R. M. Fleming, F. A. Thiel, and R. C. Haddon, *Nature* **355**, 529 (1992).

<sup>90</sup>A. R. Kortan, N. Kopylov, S. Glarum, E. M. Gyorgy, A. P. Ramirez, R. M. Fleming, O. Zhou, F. A. Thiel, P. L. Trevor and R. C. Haddon, *Nature* **360**, 566 (1992).

<sup>91</sup>R. C. Haddon, G. P. Kochanski, A. F. Hebard, A. T. Fiory, and R. C. Morris, *Science* **258**, 1636 (1992).



diffusion are critical to the preparation of high quality alkaline earth metal-doped  $C_{60}$  materials. Here we discuss approaches that have been successfully used to prepare Ca- and Ba-doped  $C_{60}$  superconductors.

The first report of an alkaline earth metal-doped  $C_{60}$  superconductor was made by Kortan and coworkers, who found a single superconducting phase with a stoichiometry of  $Ca_5C_{60}$ .<sup>89</sup> This material was prepared by pressing stoichiometric mixtures of Ca and  $C_{60}$  into pellets within tantalum cells, sealing the cells in quartz tubes under high vacuum, and then heating the reaction tubes at temperatures between 500 and 600°C. The reaction temperatures required for doping  $C_{60}$  with Ca can be compared with the much lower temperatures, 200–350°C, used for the vapor phase doping of  $C_{60}$  with K or Rb. The success of the Ca-doping reaction is due to the enhanced solid state diffusion resulting from the use of pressed pellet samples (vs. loose powders) and relatively high reaction temperatures. In principle, it would be possible to increase the solid state diffusion rates further by carrying out these intercalation reactions at even higher temperatures; however, increased reaction temperatures may also lead to the decomposition of  $C_{60}$  itself.

Similar procedures have also been used by Kortan *et al.* to prepare a barium-doped  $C_{60}$  superconductor that has a stoichiometry of  $Ba_6C_{60}$ .<sup>90</sup> An interesting structural feature of this material is that it forms a bcc lattice in contrast to all of the known alkali metal-doped superconductors. Unfortunately, the preparation of this new Ba-doped material appears to be even more difficult than  $Ca_5C_{60}$ . Briefly, extensively mixed powders of Ba and  $C_{60}$  were pressed into pellets in tantalum cells within an inert atmosphere glove box, the tantalum cells were sealed within quartz tubes at  $10^{-6}$  torr, and then these reaction vessels were heated at temperatures up to 800°C. Interestingly, reactions carried out below 600°C were found to be irreproducible, and even at higher temperatures the yields of superconducting phase are generally low. We believe that these results underscore the need for alternative approaches to prepare intercalated  $C_{60}$  solids with high melting point metals. Additionally, it is also possible that other  $C_{60}$  superconductors may be discovered as new doping procedures are developed.

## 9. NEW DIRECTIONS

The alkali and alkaline earth metal-doped  $C_{60}$  superconductors are fascinating families of superconductors. Diversity in these materials is, however, limited since their structures and properties are determined by the sizes and charges of the metal dopants. There are several possible

approaches that have been (or might be) used to expand the range of fullerene superconductors. Zhou and coworkers at Bell Laboratories have recently reported that ammonia ( $\text{NH}_3$ ) can be cointercalated into alkali metal-doped  $\text{C}_{60}$  to produce new superconducting materials.<sup>92</sup> In these studies it was found that  $\text{NH}_3$  may be absorbed by fcc  $M_3\text{C}_{60}$  compounds. Structural analysis of these materials suggests that the ammonia molecules tetrahedrally coordinate the alkali metal in the octahedral site of the fcc lattice, and thus cointercalation of  $\text{NH}_3$  represents a method by which the effective size of the alkali metal dopants can be tuned. This new method may thus help to further understanding of superconductivity in the  $M_3\text{C}_{60}$  superconductors. More generally, cointercalation represents an approach that could lead to other new fullerene superconductors. For example, ammonia should also cointercalate into the alkaline earth-doped materials, and furthermore, it may also be possible to intercalate substituted amines (e.g.,  $\text{CH}_3\text{NH}_2$ ) that have different sizes and electron affinities.

Finally, it will also be worthwhile to explore  $\text{C}_{60}$  solids doped with metals such as lanthanum and with two different metals, since these intercalation compounds could lead to materials with new structures and band fillings. Such changes may be needed to discover new fullerene solids with significantly different properties. Since the melting points of metals such as lanthanum are quite high, the development of new doping procedures to facilitate the exploration of these new systems will be necessary.

#### IV. New Fullerene Building Blocks

In the preceding sections we have reviewed the preparation of well-known fullerene clusters. Now we will introduce other carbon-based building blocks that have not been purified in macroscopic quantities. Although these materials cannot yet be used to prepare new solids, they do warrant consideration as potentially important building blocks for the future.

##### 10. ENDOHEDRAL METAL FULLERENES

Another general approach for that could be used to prepare doped fullerene solids involves encapsulating the metal dopant(s) within the

<sup>92</sup>O. Zhou, R. M. Fleming, D. W. Murphy, M. J. Rosseinsky, A. P. Ramirez, R. B. van Dover, and R. C. Haddon, *Nature* **362**, 433 (1993).

interior of the fullerene cluster. There are several features of metal encapsulated fullerenes that make these clusters important to consider for new materials research. First, encapsulated metal dopants are protected from reaction with environmental species such as oxygen and water and thus should be more stable than solids prepared by interstitial doping. Second, solids prepared from metal encapsulated fullerenes have a greater potential for diversity than is possible when doping is restricted to specific interstitial holes within the lattice. To explore the properties of solids based on metal encapsulated fullerenes requires the availability of macroscopic quantities of purified material. There are several approaches that can now be used to prepare metal encapsulated fullerenes, although methods to purify macroscopic quantities of these clusters have not been reported. Here we review the status of this work.

Metal encapsulated fullerenes were first detected in the mass spectra obtained from laser vaporization of lanthanum-, potassium-, and cesium-impregnated carbon rods.<sup>7,10</sup> More recently, the arc vaporization method of Krätschmer and Huffman has been applied to the preparation of macroscopic quantities of metal encapsulated fullerenes.<sup>43,93-100</sup> Application of this latter method simply requires that metal be incorporated into the graphite rods prior to the vaporization process; several methods have been used for this purpose. First, mixtures of metal oxide (e.g.,  $\text{La}_2\text{O}_3$ ), graphite powder, and graphite cement have been packed into holes drilled in graphite rods, and then heated from 200 to 1000°C.<sup>94-96,99,100</sup> This procedure yields mechanically robust and conducting rods that can be readily vaporized in an arc reactor. We believe, however, that it is difficult to investigate systematically the preparation of metal encapsulated fullerenes using this method, since the carbon-metal distribution is

<sup>93</sup>Y. Chai, T. Guo, C. Jin, R. E. Haufler, L. P. F. Chibante, J. Fure, L. Wang, J. M. Alford, and R. E. Smalley, *J. Phys. Chem.* **95**, 7564 (1991).

<sup>94</sup>M. M. Alvarez, E. G. Gillan, K. Holczer, R. B. Kaner, K. S. Min, and R. L. Whetten, *J. Phys. Chem.* **95**, 10561 (1991).

<sup>95</sup>M. M. Ross, H. H. Nelson, J. H. Callahan, and S. W. McElvany, *J. Phys. Chem.* **96**, 5231 (1992).

<sup>96</sup>E. G. Gillan, C. Yeretizian, K. S. Min, M. M. Alvarez, R. L. Whetten, and R. B. Kaner, *J. Phys. Chem.* **96**, 6869 (1992).

<sup>97</sup>H. Shinohara, H. Sato, M. Ohkohchi, Y. Ando, T. Kodama, T. Shida, T. Kato, and Y. Saito, *Nature* **357**, 52 (1992).

<sup>98</sup>R. D. Johnson, M. S. de Vries, J. Salem, D. S. Bethune, and C. S. Yannoni, *Nature* **355**, 239 (1992).

<sup>99</sup>L. Soderholm, P. Wurz, K. R. Lykke, D. H. Parker, and F. W. Lytle, *J. Phys. Chem.* **96**, 7153 (1992).

<sup>100</sup>H. Shinohara, H. Sato, Y. Saito, M. Ohkhchi, and Y. Ando, *J. Phys. Chem.* **96**, 3571 (1992).

very inhomogeneous in these rods. A second approach that yields a much more homogeneous mixture of metal and carbon involves forming carbon rods from intimate mixtures of metal oxide, graphite powder, and graphite cement in a metal die.<sup>93,97,98</sup> The rods obtained after initial curing of the graphite cement are poorly conducting and mechanically fragile, and thus they are unsuitable for arc vaporization. Vacuum annealing at high temperature (1000–1200°C), however, does produce conducting rods that are mechanically robust.

Metal-carbon rods obtained using the foregoing procedures have been used to prepare a variety of metal encapsulated fullerenes, including (1) metallofullerenes  $MC_{82}$  ( $M = \text{Sc}, \text{Y}$ , and the lanthanides) containing a single metal ion; (2) the dimetallofullerenes  $\text{La}_2\text{C}_{80}$  and  $\text{Y}_2\text{C}_{82}$ ; and (3) the trimetallofullerene  $\text{Sc}_3\text{C}_{82}$ .<sup>93–100</sup> In general, the primary characterization method used to identify these metal encapsulated fullerene materials has been mass spectroscopy analysis of the soot obtained from arc vaporization of the metal-carbon rods. A typical example of a spectrum obtained following vaporization of 10%  $\text{La}_2\text{O}_3$ -carbon rods is shown in Fig. 16. In this spectrum a clear peak is observed at the mass corresponding to  $\text{LaC}_{82}$  as well as peaks corresponding to other fullerenes such as  $\text{C}_{60}$  and  $\text{C}_{70}$ ; the  $\text{LaC}_{82}$  clusters represents approximately 2–5% of the total fullerene products.

These results clearly demonstrate the presence of metallofullerene

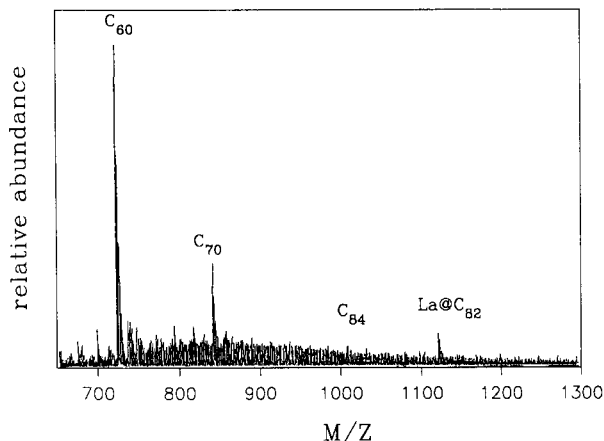


FIG. 16. Fast atom bombardment mass spectrum of the pyridine soluble extract of the soot produced by arc vaporization of lanthanum-containing graphite electrodes. The presence of the lanthanum encapsulated fullerene,  $\text{La}@\text{C}_{82}$ , is clearly evident in this spectrum.

clusters in the soot obtained from the vaporization of metal-carbon rods. The mere presence of metallofullerenes, however, does not necessarily make them useful for solid state studies. To prepare new materials based on metallofullerenes requires macroscopic quantities of the pure clusters. At present, however, there are no reported approaches that can be used to isolate pure metallofullerene clusters. Because solids based on these new clusters could yield exciting electrical, optical, or magnetic properties, it is important to consider possible ways in which large scale isolation can be achieved. First, separation would be greatly facilitated by increasing the overall yield of metallofullerene in the crude soot. Systematic studies of the relative metallofullerene to fullerene product yield as a function of the composition of the metal-carbon rods and the vaporization conditions will indicate how the yield of the desired metallofullerene clusters can be enhanced. Second, the stability of the metallofullerene clusters is not well understood at present. Because these clusters may decompose in an ambient environment (where most isolation procedures have been carried out), we believe that it would be worthwhile to investigate the purification of metallofullerenes using anaerobic conditions. Finally, the metallofullerenes are expected to be polar clusters (i.e., there is significant charge transfer from the metal to the fullerene),<sup>101</sup> and thus procedures used to isolate neutral fullerenes (e.g.,  $C_{60}$  and  $C_{70}$ ) may not be a good starting point for the isolation of metal-containing fullerenes. In this regard, chromatographic techniques that are suitable for the separation of large polar macromolecules should represent a promising avenue of investigation.

## 11. CARBON NANOTUBES

Carbon nanotubes are finite carbon structures that consist of concentric tubes of graphite sheets (Fig. 17).<sup>102-106</sup> Nanotubes differ significantly from the fullerene clusters already discussed since they possess a quasi-one-dimensional or needle like structure. These carbon tubes are, however, interesting building blocks to consider for the preparation of new solid state materials. For example, carbon nanotubes are predicted to be mechanically stiffer than any presently available carbon fiber

<sup>101</sup>K. Laasonen, W. Andreoni, and M. Parrinello, *Science* **258**, 1916 (1992).

<sup>102</sup>S. Iijima, *Nature* **354**, 56 (1991).

<sup>103</sup>T. W. Ebbesen and P. M. Ajayan, *Nature* **358**, 220 (1992).

<sup>104</sup>S. Iijima, T. Ichihashi, and Y. Ando, *Nature* **356**, 776 (1992).

<sup>105</sup>D. Ugarte, *Nature* **359**, 707 (1992).

<sup>106</sup>Z. Zhang and C. M. Lieber, *Appl. Phys. Lett.* **62**, 2792 (1993).



FIG. 17. Transmission electron micrograph of a carbon nanotube supported on an amorphous carbon grid; the micrograph shows a cross-sectional view of the tube. The nanotube has an outside diameter of 100 Å and consists of 12 concentric shells.

material.<sup>107</sup> Electronic structure calculations also predict that nanotubes will exhibit metallic or semiconducting properties depending on the diameter and helicity of the tubes.<sup>108–111</sup> These latter properties could be used to prepare solids with novel electronic and/or optical properties.

The preparation of carbon nanotubes was first reported by Iijima in 1991.<sup>102</sup> In this work it was shown that these needlelike structures were present in the deposit remaining after direct current evaporation of carbon rods in approximately 100 torr of argon. More recently, Ebbesen and Ajayan reported the development of a large scale synthesis of carbon nanotubes using a technique similar to that employed by Iijima.<sup>103</sup> Importantly, these latter investigations have demonstrated that high yields of nanotubes can be obtained when the inert gas pressure is 500 torr or greater during the vaporization process. The optimal nanotube preparation pressure is thus significantly higher than the 100–200 torr pressure that is best for fullerene formation.

To prepare homogeneous solids from these fascinating carbon tubes now requires the development of a method to separate macroscopic

<sup>107</sup>M. S. Dresselhaus, *Nature* **358**, 220 (1992).

<sup>108</sup>J. W. Mintmire, B. I. Dunlap, and C. T. White, *Phys. Rev. Lett.* **68**, 631 (1992).

<sup>109</sup>N. Hamada, S.-I. Sawada, and A. Oshiyama, *Phys. Rev. Lett.* **68**, 1579 (1992).

<sup>110</sup>R. Saito, M. Fujita, G. Dresselhaus, and M. S. Dresselhaus, *Appl. Phys. Lett.* **60**, 2204 (1992).

<sup>111</sup>R. Saito, M. Fujita, G. Dresselhaus, and M. S. Dresselhaus, *Phys. Rev. B* **46**, 1804 (1992).

quantities of nanotubes that have a uniform helicity and diameter. A significant hurdle in this regard is that the nanotubes are insoluble in organic solvents (in contrast to the fullerenes) and thus cannot be separated using standard chromatographic techniques. Several alternative strategies that might lead to advances in this separation problem include the following. First, variations in the current density and rate of carbon vaporization might lead to better control of the nanotube size distribution. Control of the size distribution could significantly reduce the difficulty of any purification process. Second, it may be possible to chemically functionalize or modify the nanotubes to facilitate separation and isolation. One interesting example of chemical modification involves the recently reported reactions of nanotubes with  $O_2$  and  $CO_2$  at elevated temperature.<sup>112,113</sup> In these studies it was found that either molecular species reacts with the tubes to remove the outer concentric carbon shells. Since the smallest inside shells of many nanotubes are the same, these reactions could be used to convert a crude mixture of material into relatively homogeneous nanotube samples. Finally, it is also interesting that Ajayan and Iijima have observed that heating nanotubes in the presence of liquid metals such as Pb results in the filling of the tubes with the metal.<sup>114</sup> Because Pb becomes superconducting at approximately 7 K, it would be possible to separate Pb-filled and virgin nanotubes magnetically at liquid helium temperatures. Since metal filling depends on the interior size of the tube, this approach could also lead to a technique for preparing homogeneous nanotube samples. Lastly, we expect that the metal nanotube species may constitute especially interesting building blocks for the preparation of new materials.

## V. Concluding Remarks

In this chapter we have concentrated primarily on reviewing the preparation, isolation, and characterization of fullerene clusters, and the preparation of new solids based on these closed carbon clusters. This review has been done at a level such that physicists and chemists can now carry out experimental research in this field starting only from carbon rods. In the first part of the chapter, the relative merits and shortcomings of well-established techniques for preparing fullerenes from carbon rods,

<sup>112</sup>S. C. Tsang, P. J. F. Harris, and M. L. H. Green, *Nature* **362**, 520 (1993).

<sup>113</sup>P. M. Ajayan, T. W. Ebbesen, T. Ichihashi, S. Iijima, K. Tanigaki, and H. Hiura, *Nature* **362**, 522 (1993).

<sup>114</sup>P. M. Ajayan and S. Iijima, *Nature* **361**, 333 (1993).

isolating pure fullerenes, and characterizing the purity of these materials were discussed. These sections focused on developing efficient strategies to prepare and assess the purity of  $C_{60}$  since this cluster remains the most widely used building block for solids. Efficient and general approaches for preparing isotopically substituted fullerenes, which are essential materials for solid state research, were also discussed in this section. In the second major section of this chapter, we reviewed the properties of solid  $C_{60}$  and methods for preparing metal-doped  $C_{60}$  solids. This part of the review, which concentrated primarily on fullerene superconductors, provides readers with sufficient information to enter this fascinating area of condensed matter physics where a number of fundamental issues remain to be defined (e.g., see the chapter on fullerene superconductivity). Finally, in the last section of the chapter the prospects for materials based on two new carbon building blocks, metallofullerenes and nanotubes, were explored. While well-defined solids built up from metallofullerenes or nanotubes are not yet available, such materials could in the future provide a revolutionary advance in materials research as the discovery and preparation of copper oxide and  $C_{60}$  solids have done in the recent past.